Polarimetric modeling of brown dwarf atmospheres

Suniti Sanghavi

Jet Propulsion Laboratory, CA
Copyright 2019 California Institute of Technology.
Government sponsorship acknowledged.

sanghavi@jpl.nasa.gov

Jan 9, 2019

Outline

Table of Contents

Need for brown dwarf (BD) modeling

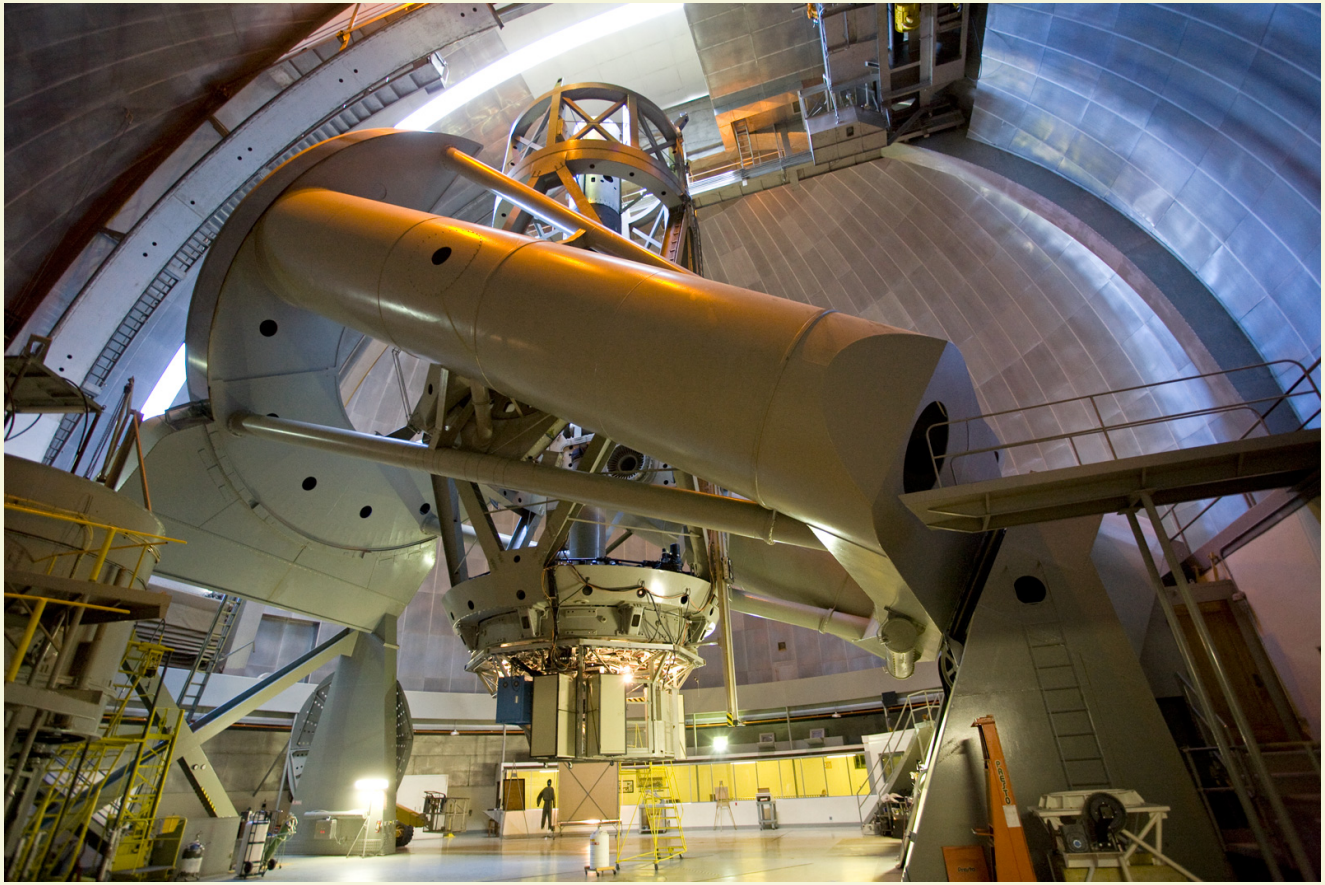

- WIRC+Pol team currently involved in a spectro-polarimetric survey of over 100 BDs and EGPs using 200" Hale telescope on Mt. Palomar

Table of Contents

Need for brown dwarf (BD) modeling

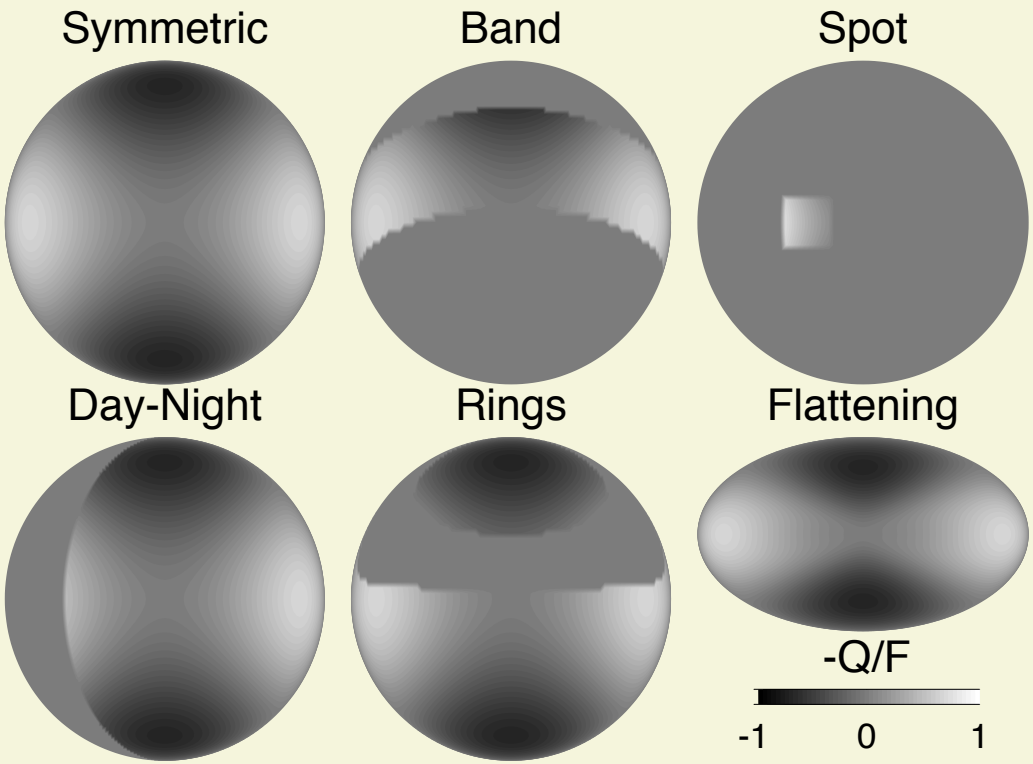

(de Kok et al. 2011)

- Polarimetry makes BD measurements sensitive to asymmetric features like oblateness and patchy clouds

Need for brown dwarf (BD) modeling: oblateness

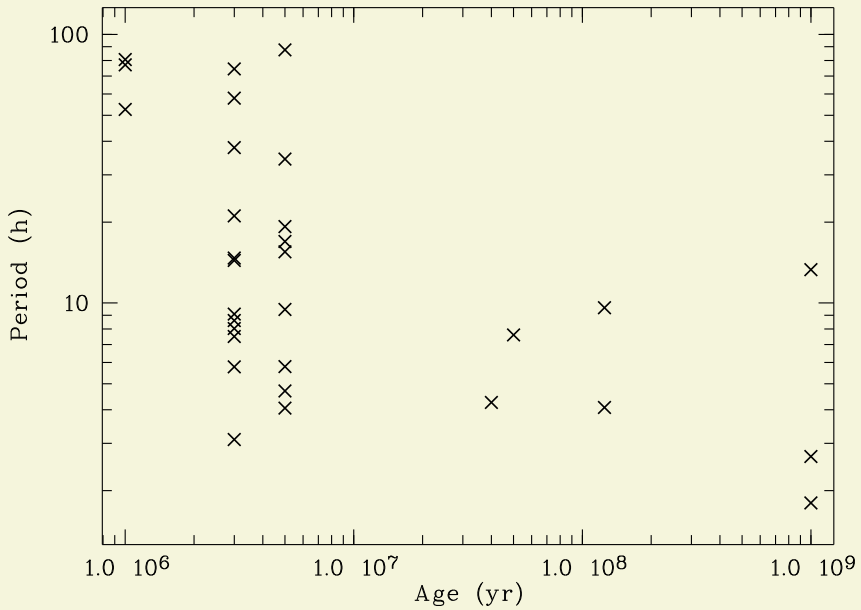

(Herbst et al., Scholz & Eislöffel 2004)

- L-dwarfs (∼2200-1600 K) and T-dwarfs (∼1600-500 K) have undergone radiative cooling with age (~ 1 Gyr), shrinking to the size of Jupiter.
- Lack of efficient braking mechanisms causes them to conserve momentum by spinning increasingly faster, so that some BDs approach the Roche break-up limit

Need for brown dwarf (BD) modeling: oblateness

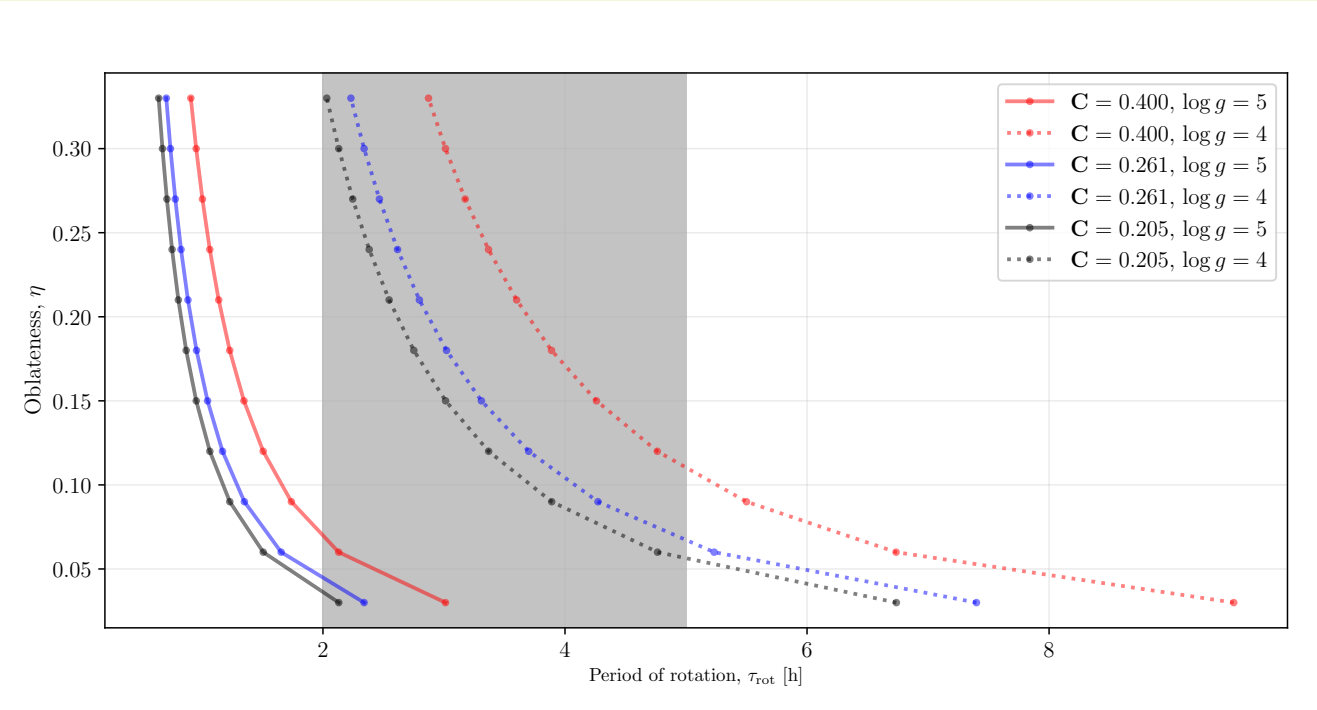

- Many brown dwarfs have a period of rotation between 2-5 hrs, covering the full range of oblateness between $\eta = 0 - 0.33$

Need for brown dwarf (BD) modeling: patchy clouds

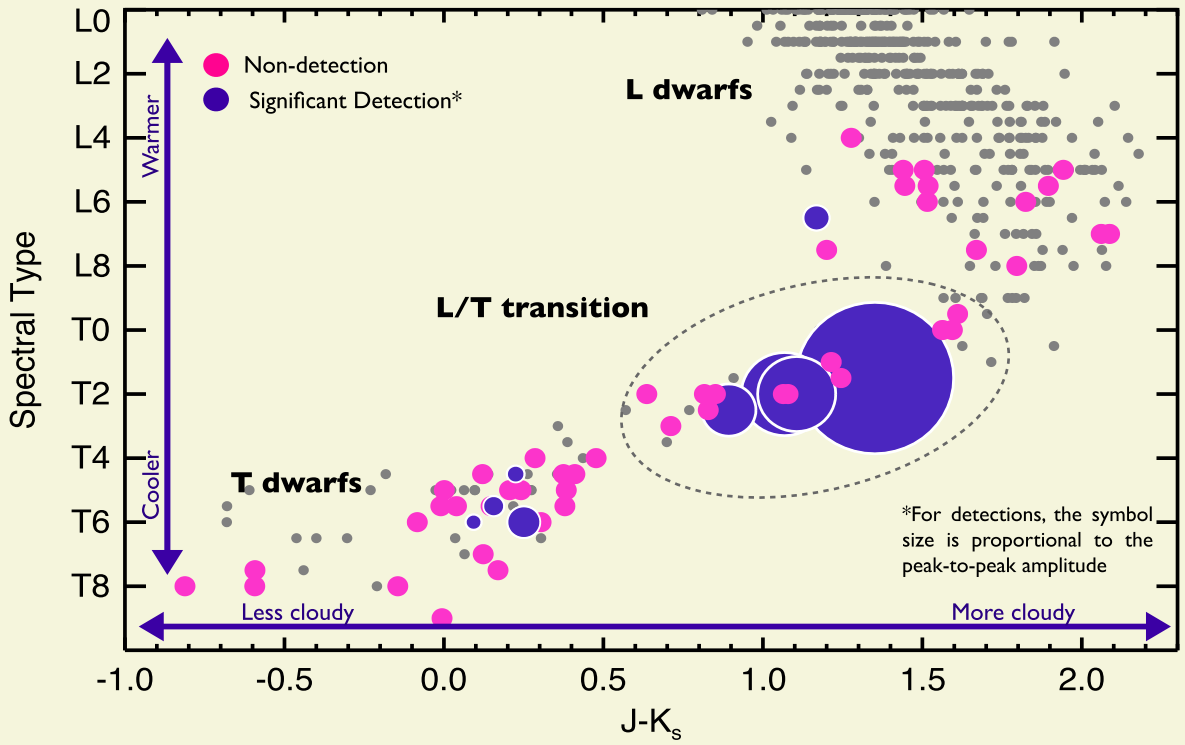

(Radigan et al. 2014)

- Late L- and early T-dwarfs start seeing the fragmentation and precipitation of clouds near the photosphere, revealing deeper layers of the atmosphere

Need for brown dwarf (BD) modeling: patchy clouds

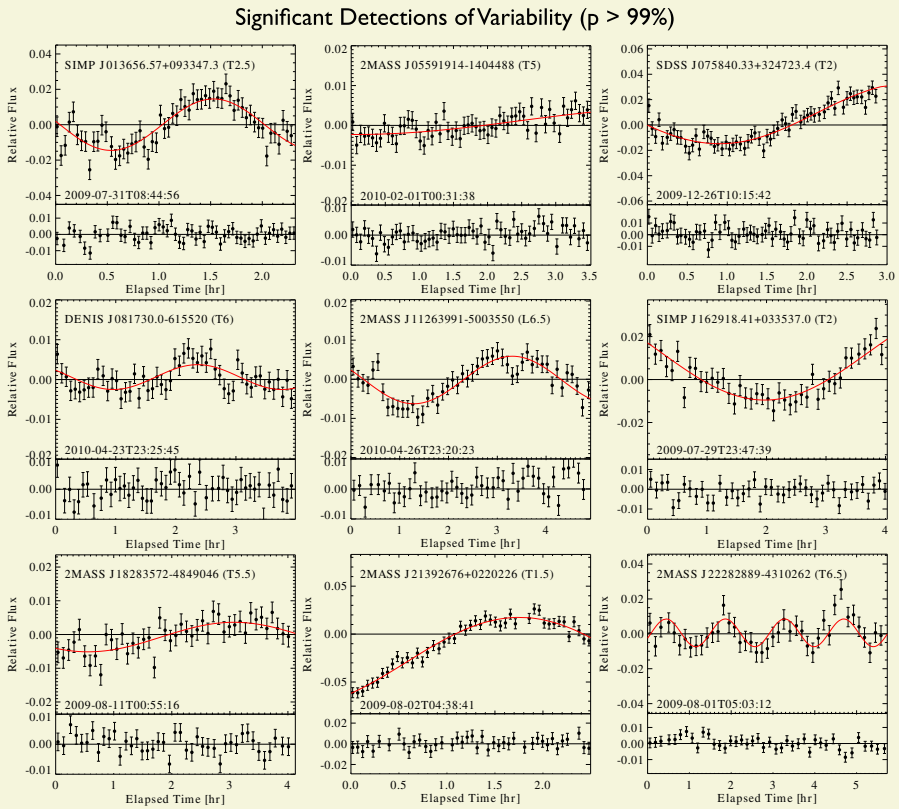

(Radigan et al. 2014)

- High quality observations of photometric variability confirm patchy clouds to be a dominant feature of BDs in L/T-transition

Table of Contents

Need of a framework to model oblate BDs with patchy clouds

- Conics-based semi-analytical 3D framework using the 1D polarized RTM vSmartMOM (Sanghavi et al. 2014)
- Fast and accurate modeling of scattering by distributions of spherical cloud grains (Sanghavi 2014, Sanghavi et al. 2015)
- Provides simultaneous, polarized simulations of oblateness and any number of cloud patches at a given inclination angle (Sanghavi & Shporer 2018, henceforth SS18)

Preliminary assumptions

- For generality, we assumed in SS18 a gray atmosphere, so that the BD emits as a black body of temperature $T_{\rm eff}$.
- To estimate the spectral variations in photospheric depth due to atmospheric opacities, we assumed two limiting cases:
  1. A completely non-absorbing atmosphere, for which the photosphere is at the bottom of the atmospheric (gaseous) column (BOA)
  2. An almost completely opaque atmosphere, for which the photosphere is practically at the top of atmosphere (TOA)
- The modeled cloud consists of a log-normal distribution of spherical, Mie-scattering, silicate grains and always occurs above the photosphere

vSmartMOM: first simulations of patchy clouds on oblate BDs (Sanghavi et al., 2018)

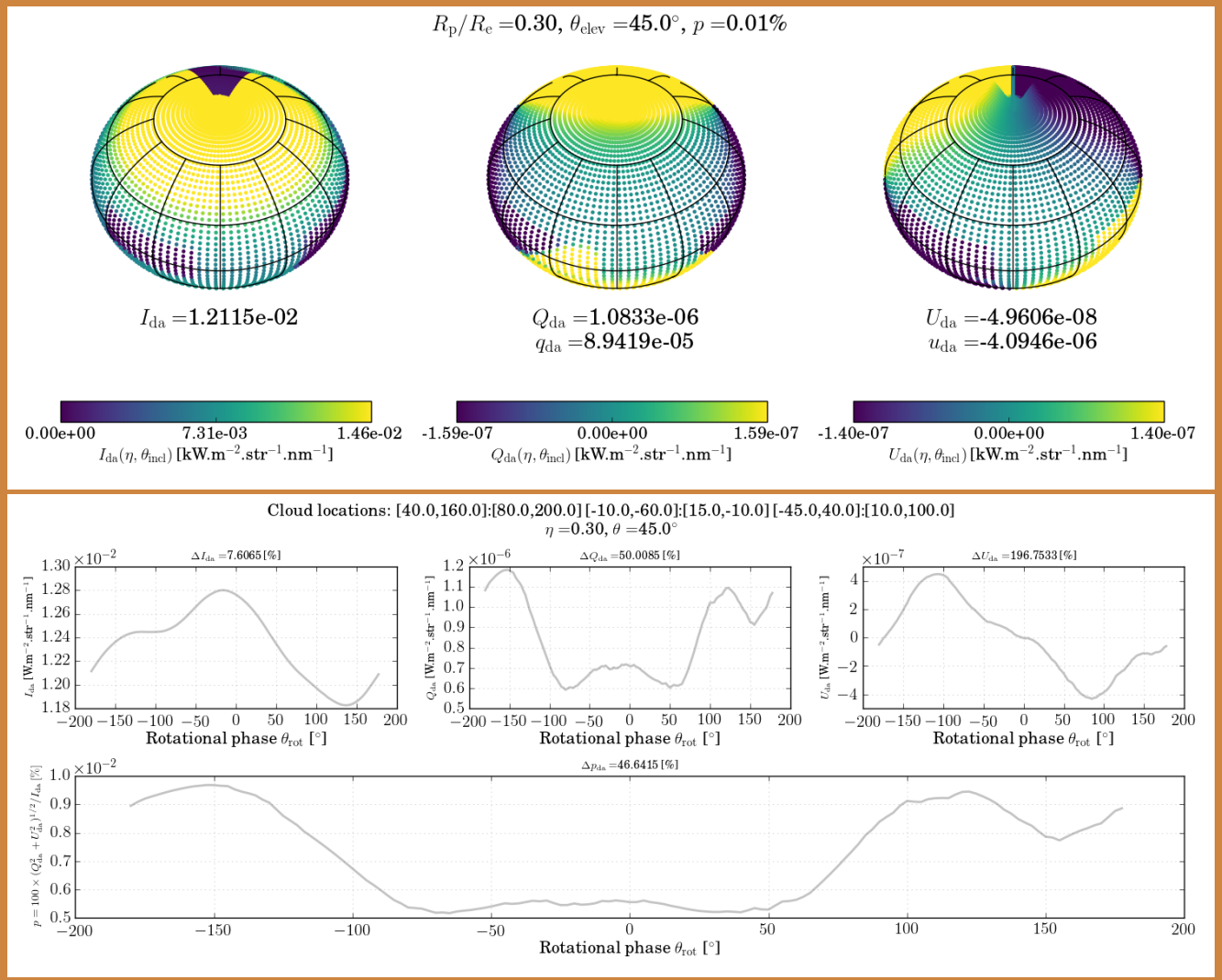

Effect of oblateness and inclination angle

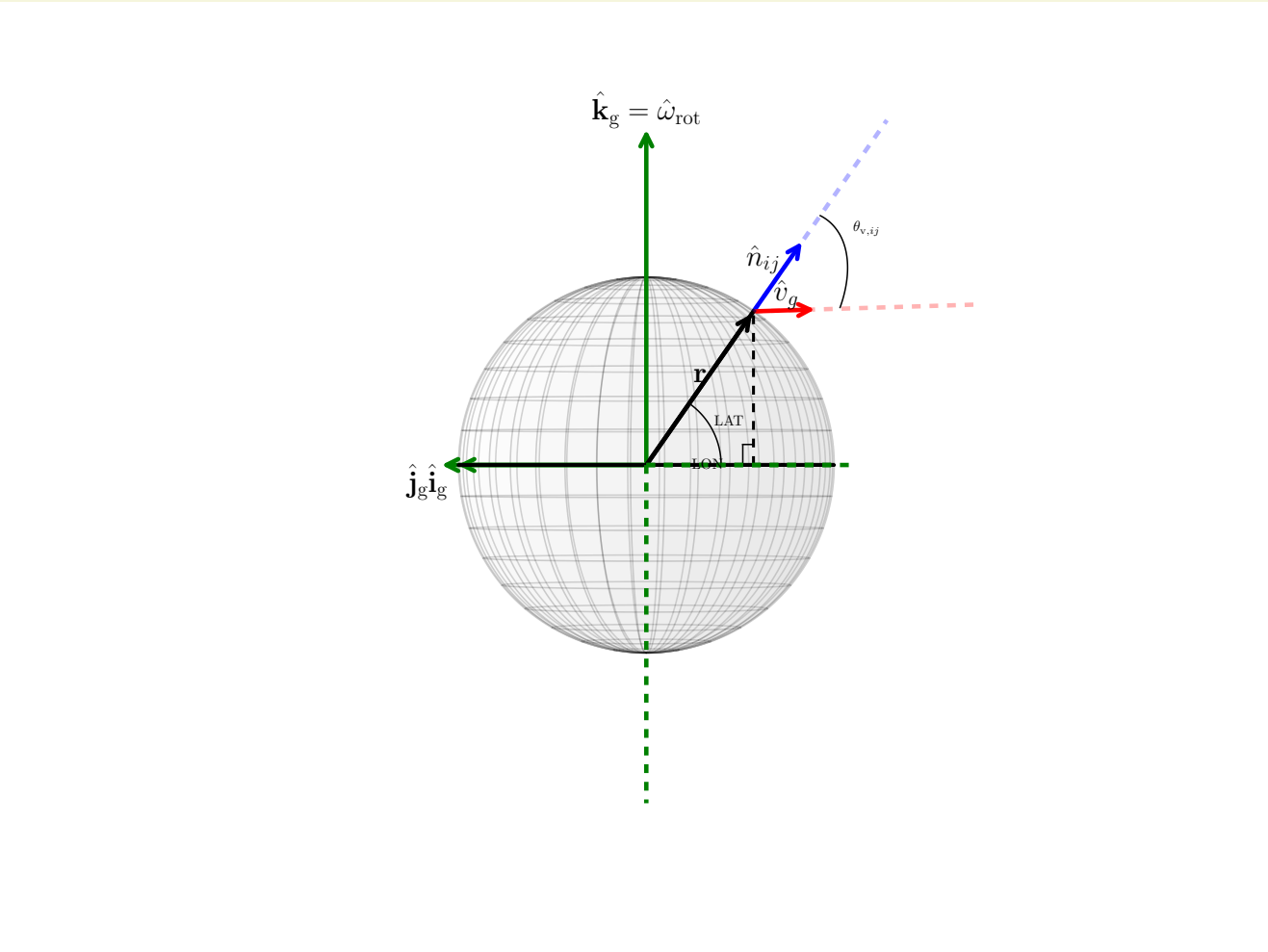

- Spherical case, η=0, unaffected by inclination angle, $\theta_{\rm incl}$
- Normal vectors $\hat{\mathbf{n}}_{ij}$ are always coincident with the unit radial vectors $\hat{\mathbf{r}}_{ij}$

Effect of oblateness and inclination angle

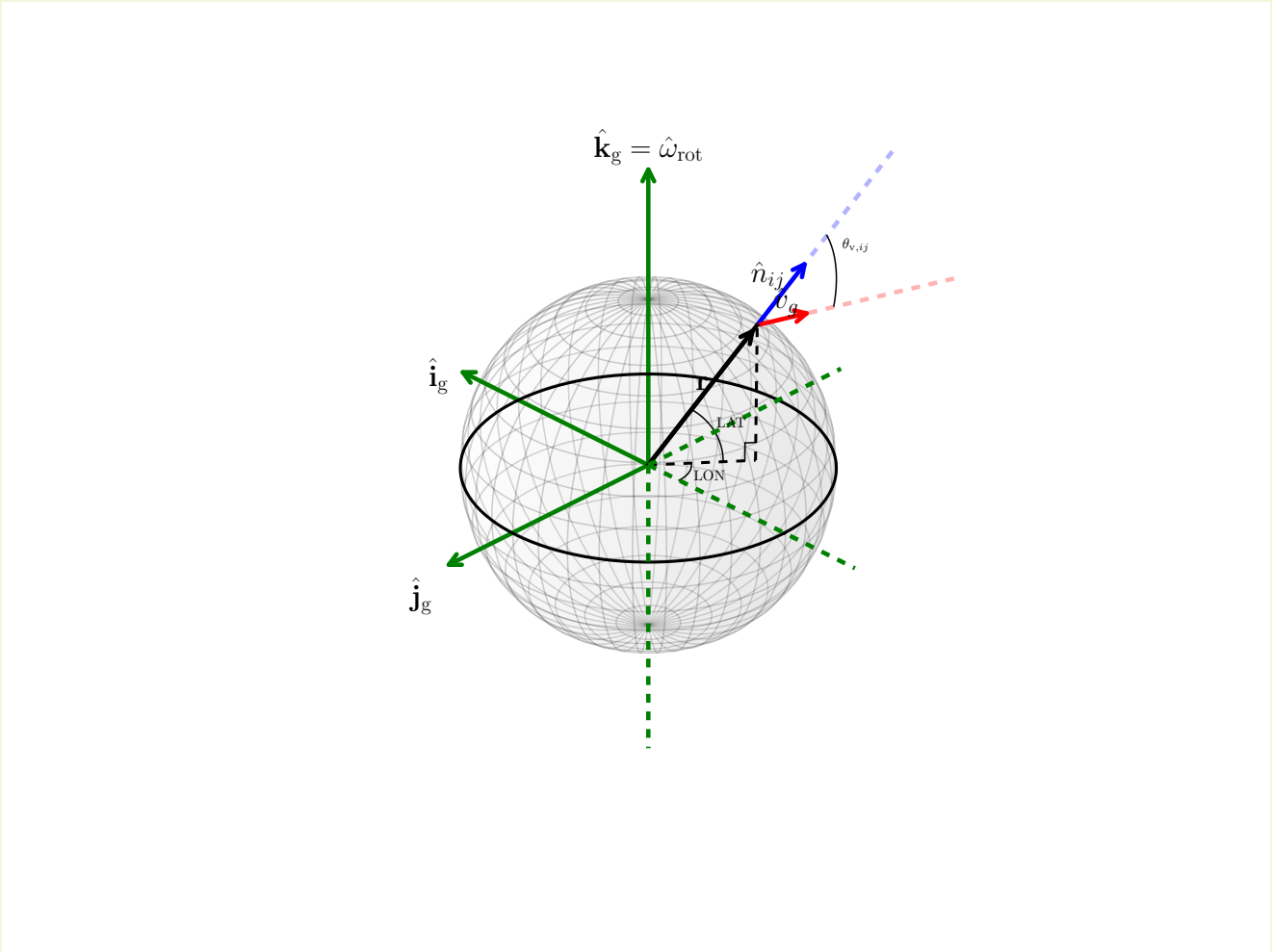

- Spherical case, η=0, unaffected by inclination angle, θ_{incl}
- Normal vectors $\hat{\mathbf{n}}_{ij}$ are always coincident with the unit radial vectors $\hat{\mathbf{r}}_{ij}$

Effect of oblateness and inclination angle

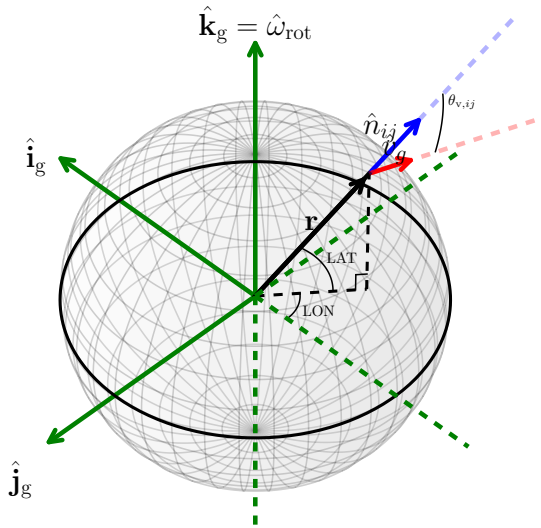

- Spherical case, η=0, unaffected by inclination angle, $\theta_{\rm incl}$
- Normal vectors $\hat{\mathbf{n}}_{ij}$ are always coincident with the unit radial vectors $\hat{\mathbf{r}}_{ij}$

Effect of oblateness and inclination angle

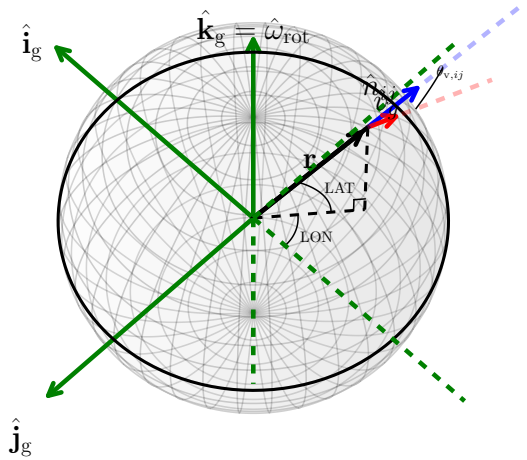

- Spherical case, η=0, unaffected by inclination angle, θ_{incl}
- Normal vectors $\hat{\mathbf{n}}_{ij}$ are always coincident with the unit radial vectors $\hat{\mathbf{r}}_{ij}$

Effect of oblateness and inclination angle

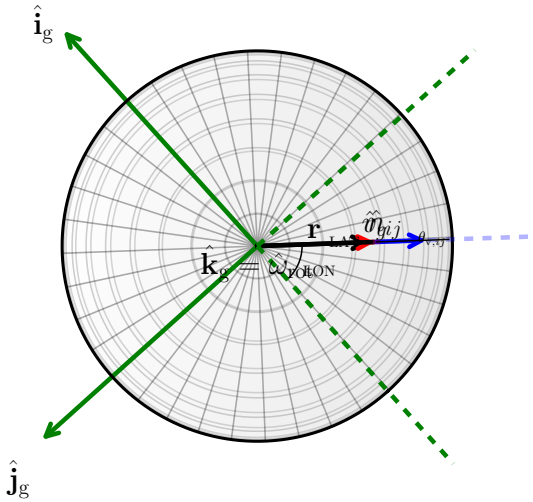

- Spherical case, η=0, unaffected by inclination angle, $\theta_{\rm incl}$
- Normal vectors $\hat{\mathbf{n}}_{ij}$ are always coincident with the unit radial vectors $\hat{\mathbf{r}}_{ij}$

Effect of oblateness and inclination angle

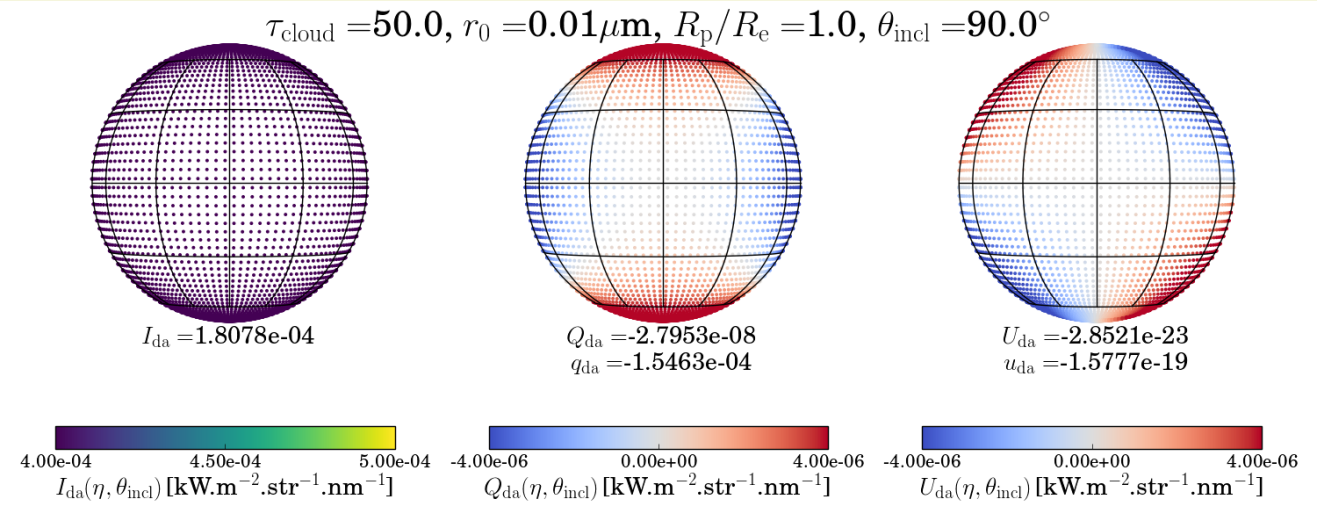

Effect of oblateness and inclination angle

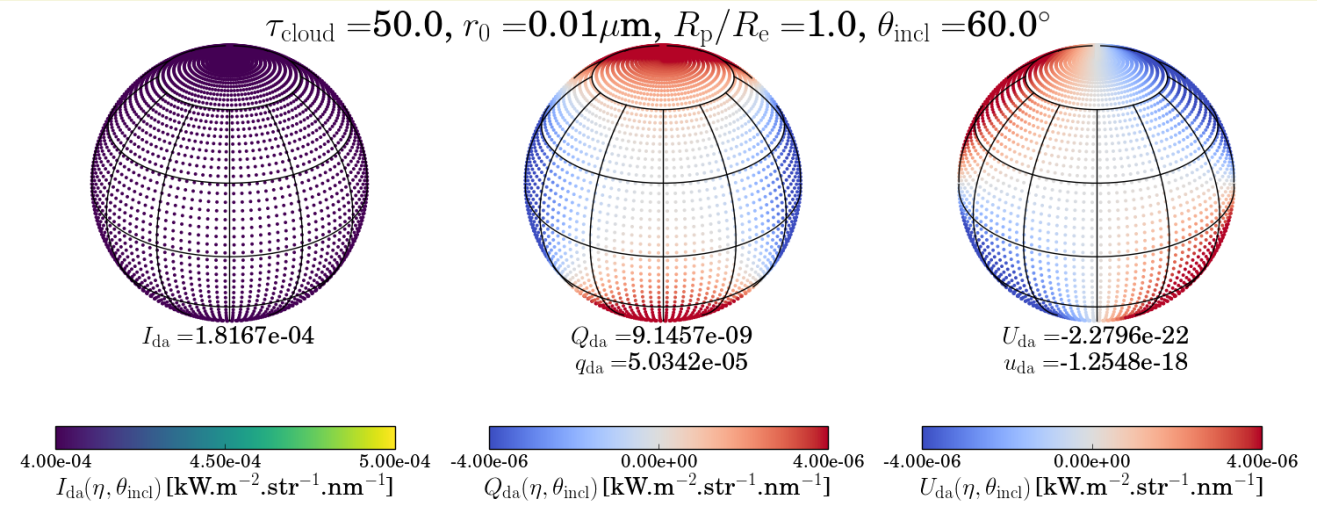

Effect of oblateness and inclination angle

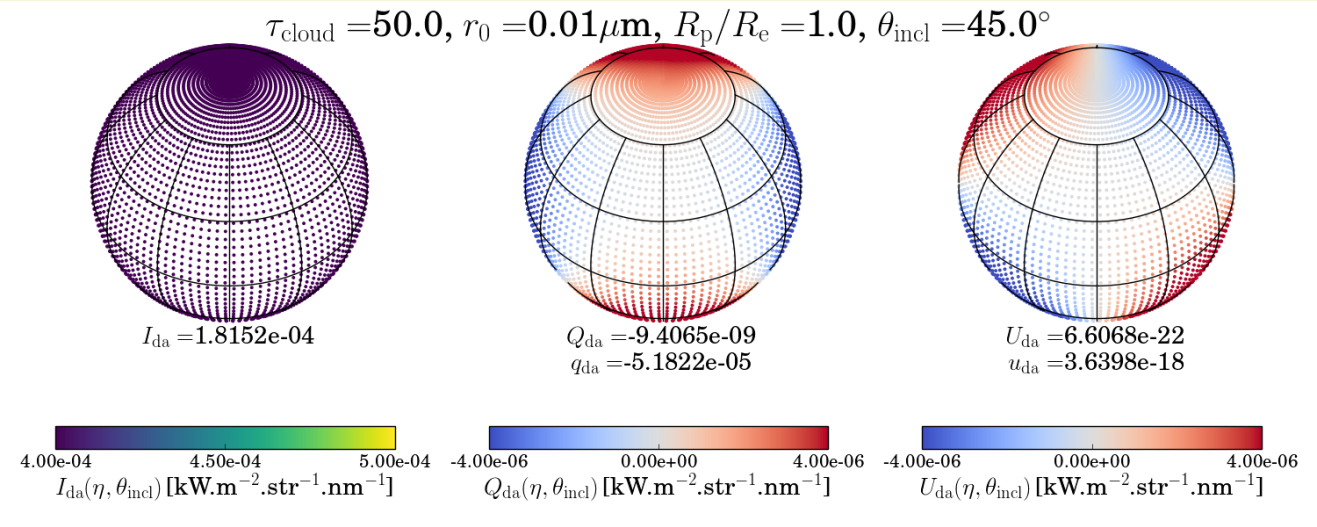

Effect of oblateness and inclination angle

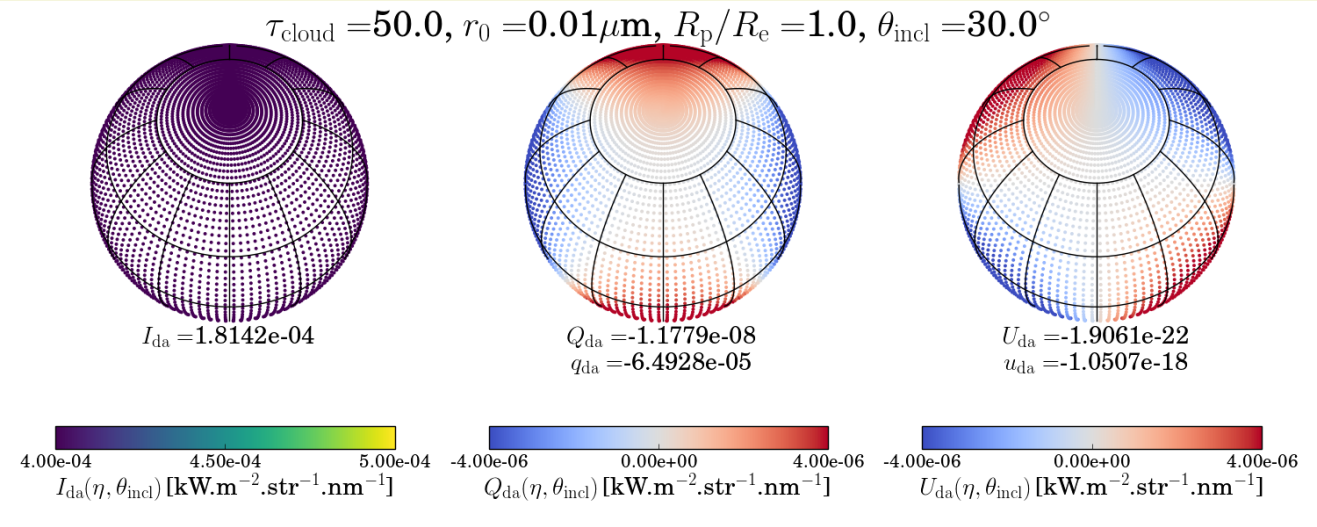

Effect of oblateness and inclination angle

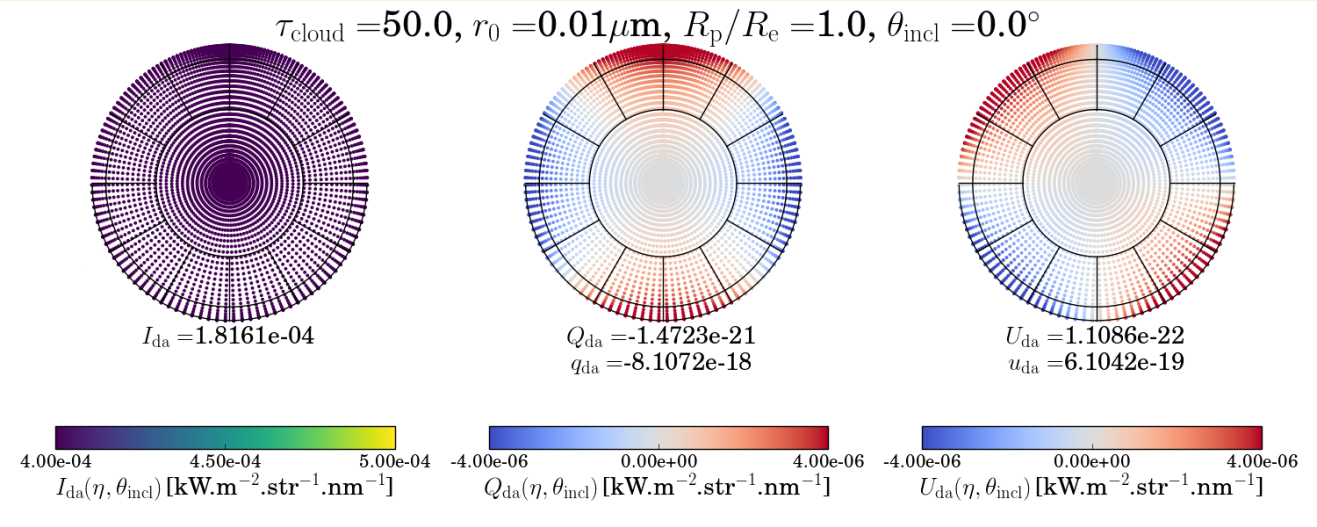

Effect of oblateness and inclination angle

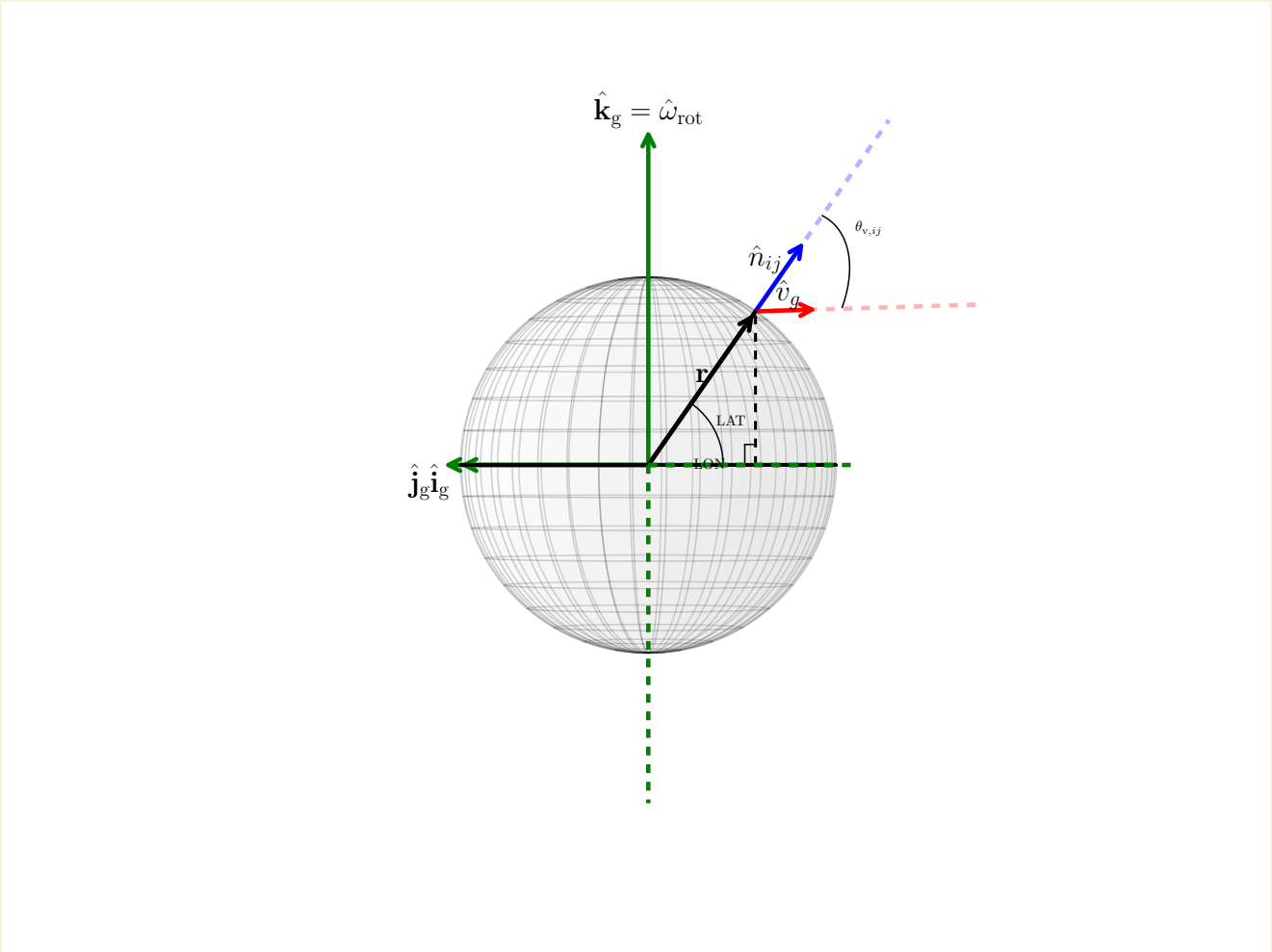

- As the BD becomes more oblate, the normal vectors $\hat{\mathbf{n}}_{ij}$ is no longer coincident with the unit radial vectors $\hat{\mathbf{r}}_{ij}$

Effect of oblateness and inclination angle

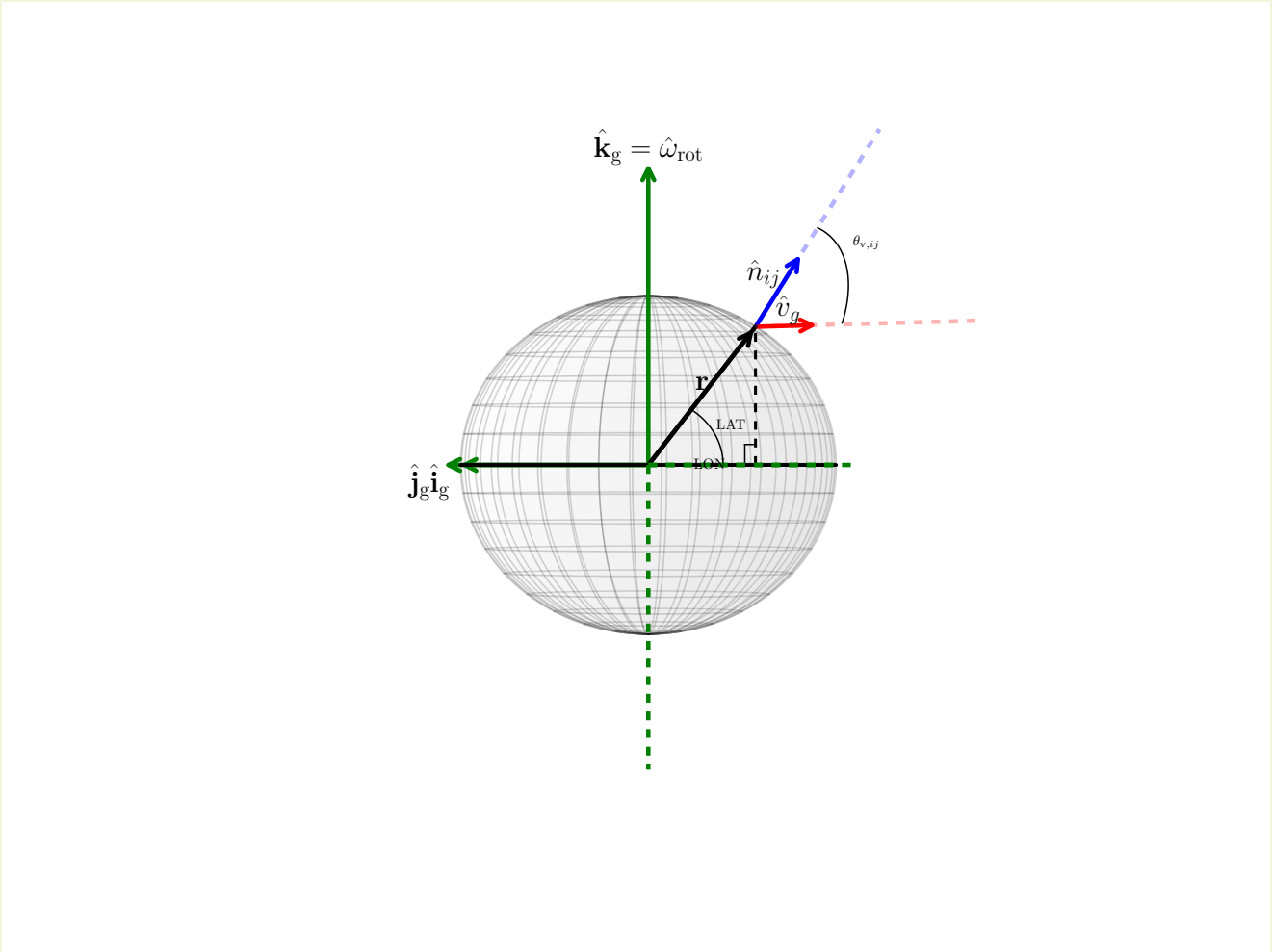

- As the BD becomes more oblate, the normal vectors $\hat{\mathbf{n}}_{ij}$ is no longer coincident with the unit radial vectors $\hat{\mathbf{r}}_{ij}$

Effect of oblateness and inclination angle

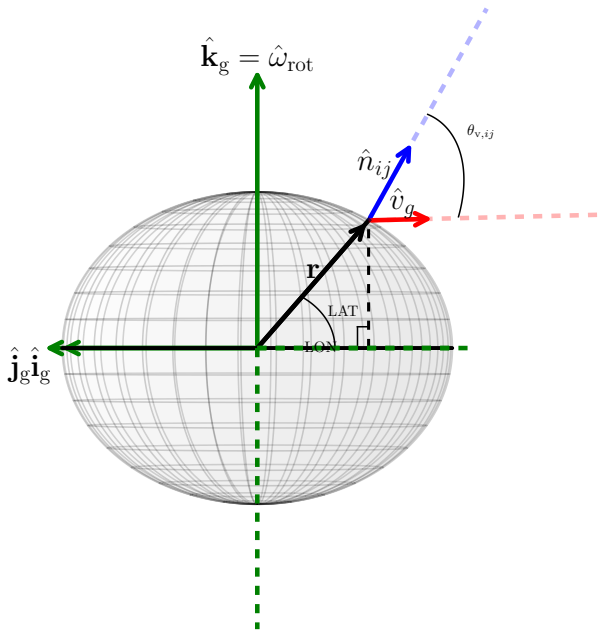

- As the BD becomes more oblate, the normal vectors $\hat{\mathbf{n}}_{ij}$ is no longer coincident with the unit radial vectors $\hat{\mathbf{r}}_{ij}$

Effect of oblateness and inclination angle

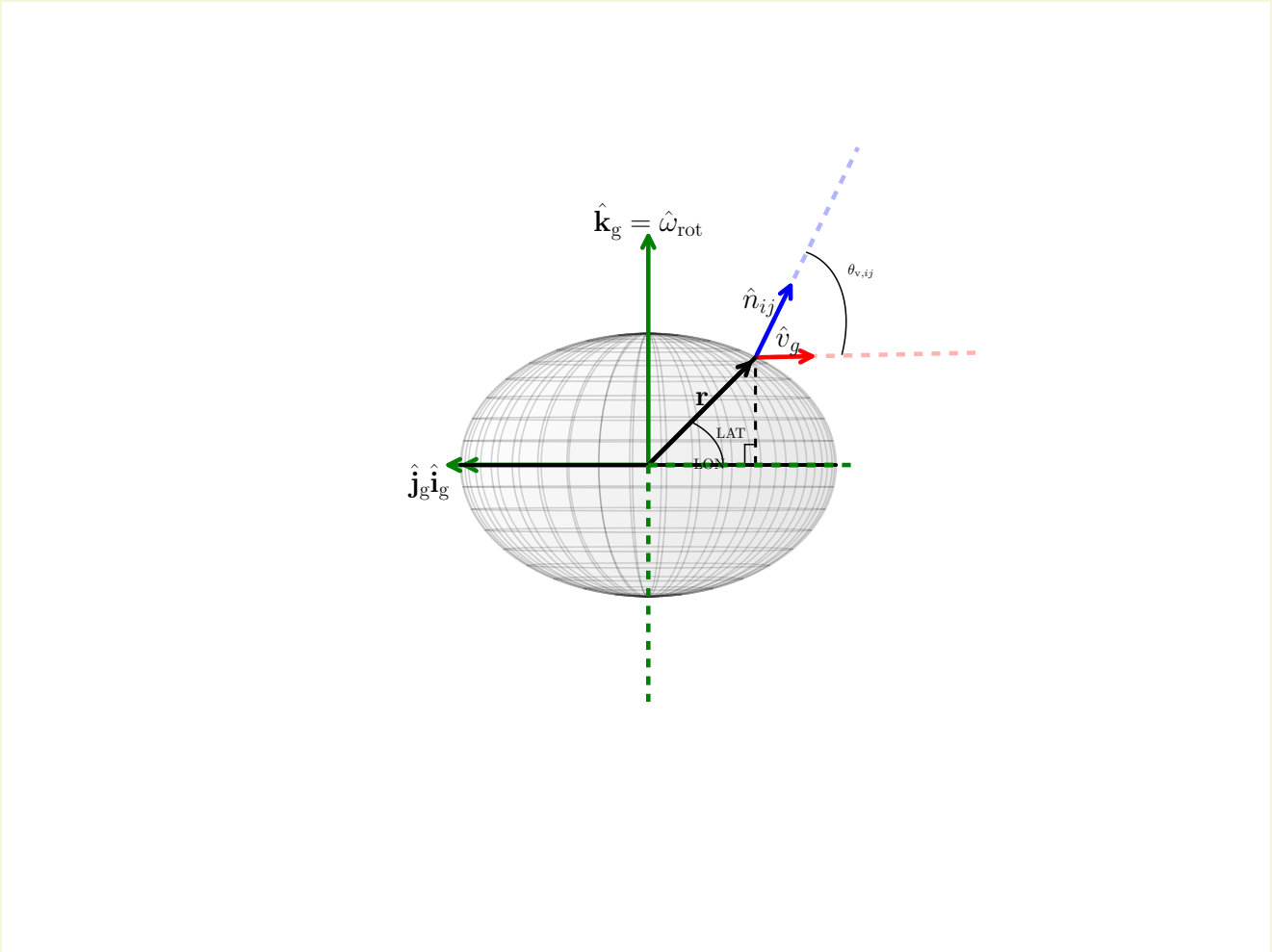

- As the BD becomes more oblate, the normal vectors $\hat{\mathbf{n}}_{ij}$ is no longer coincident with the unit radial vectors $\hat{\mathbf{r}}_{ij}$

Effect of oblateness and inclination angle

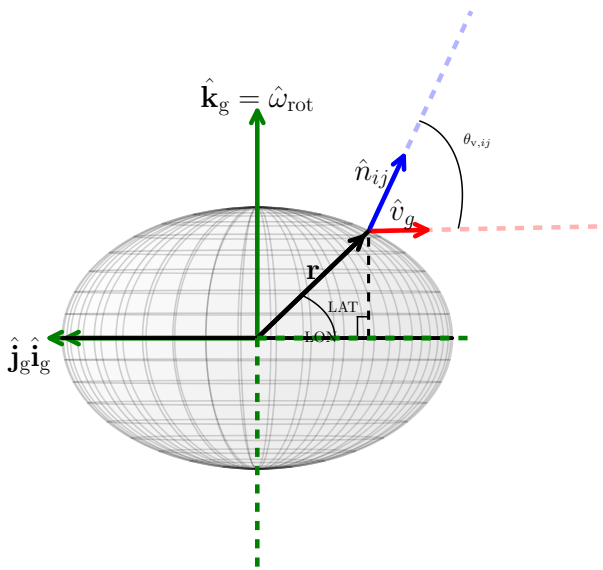

- As the BD becomes more oblate, the normal vectors $\hat{\mathbf{n}}_{ij}$ is no longer coincident with the unit radial vectors $\hat{\mathbf{r}}_{ij}$

Effect of oblateness and inclination angle

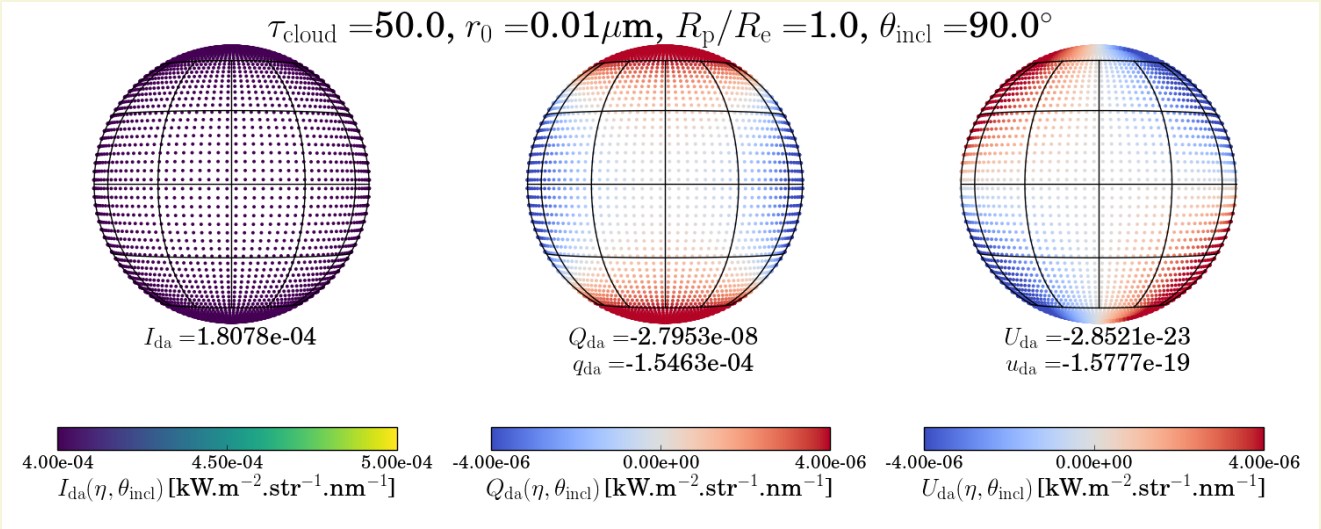

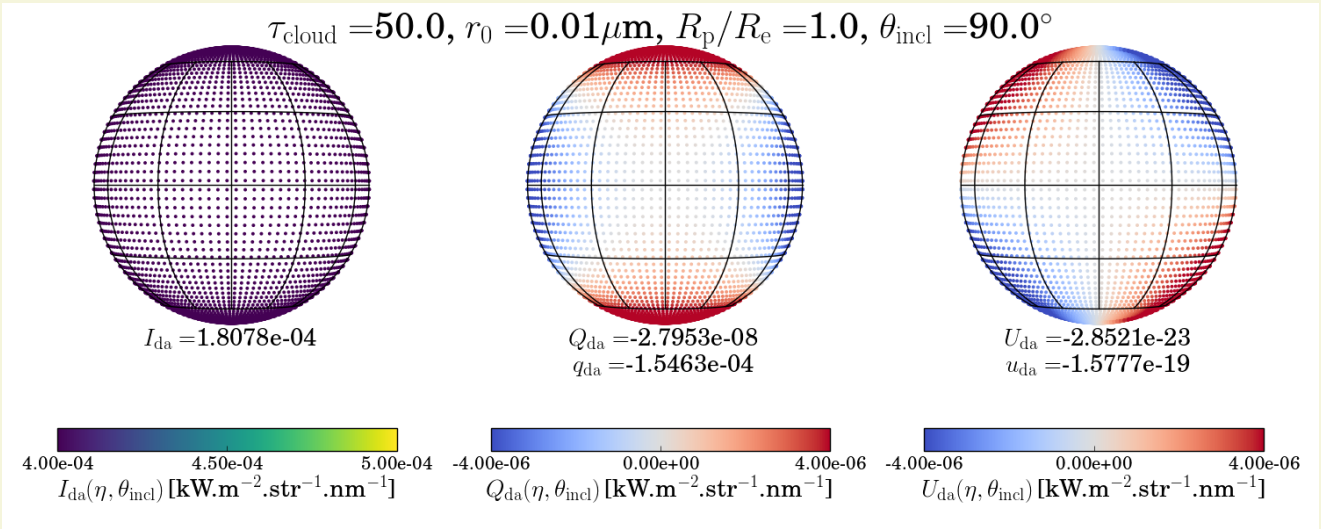

Effect of oblateness and inclination angle

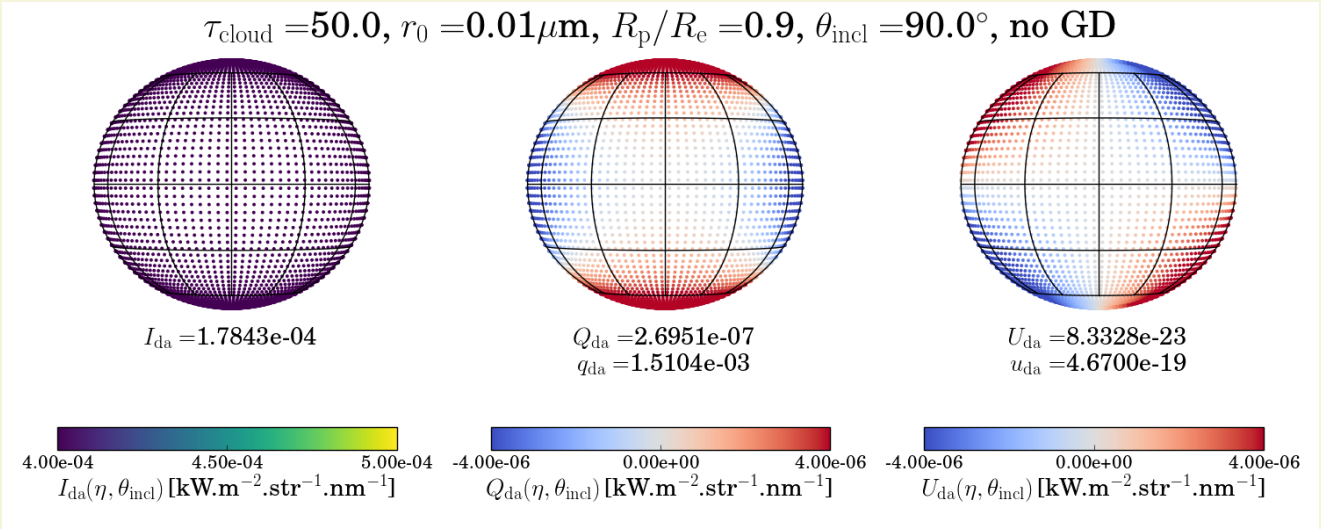

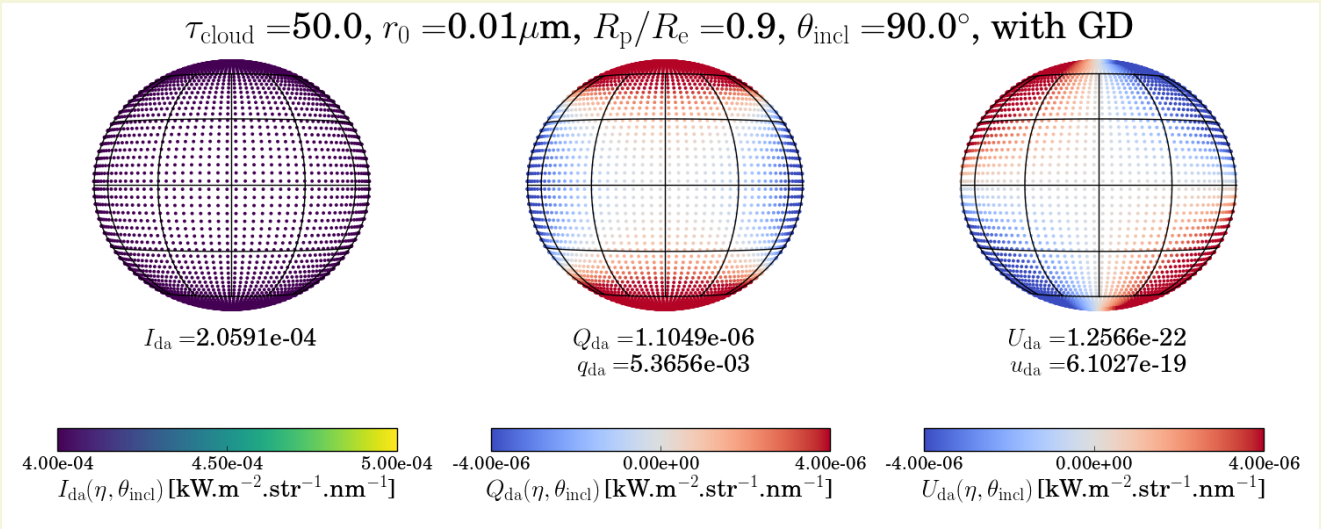

Effect of oblateness and inclination angle

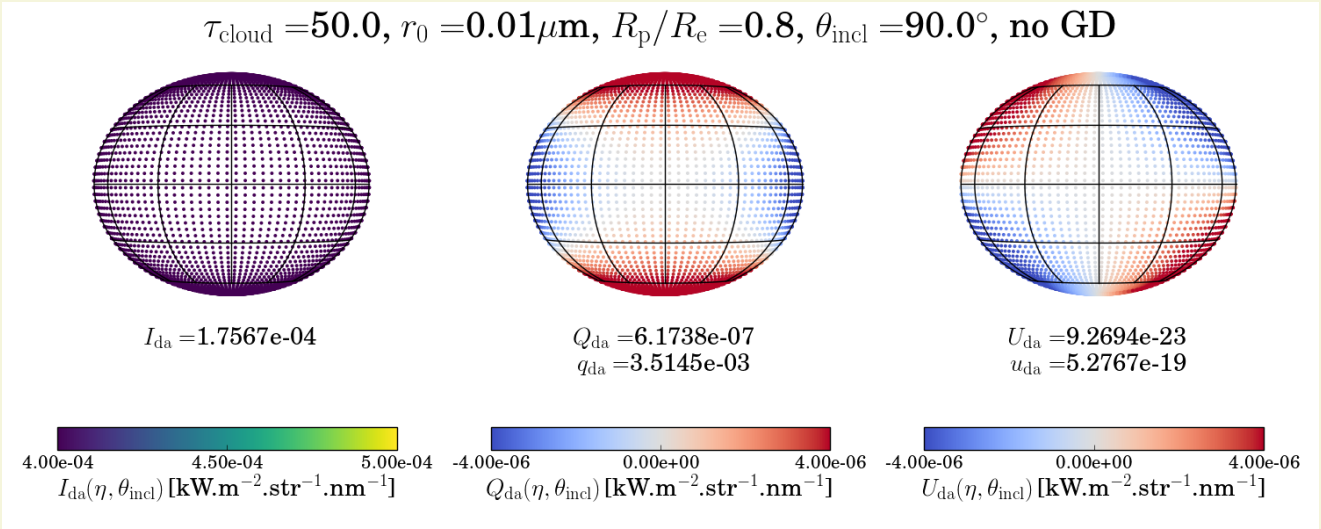

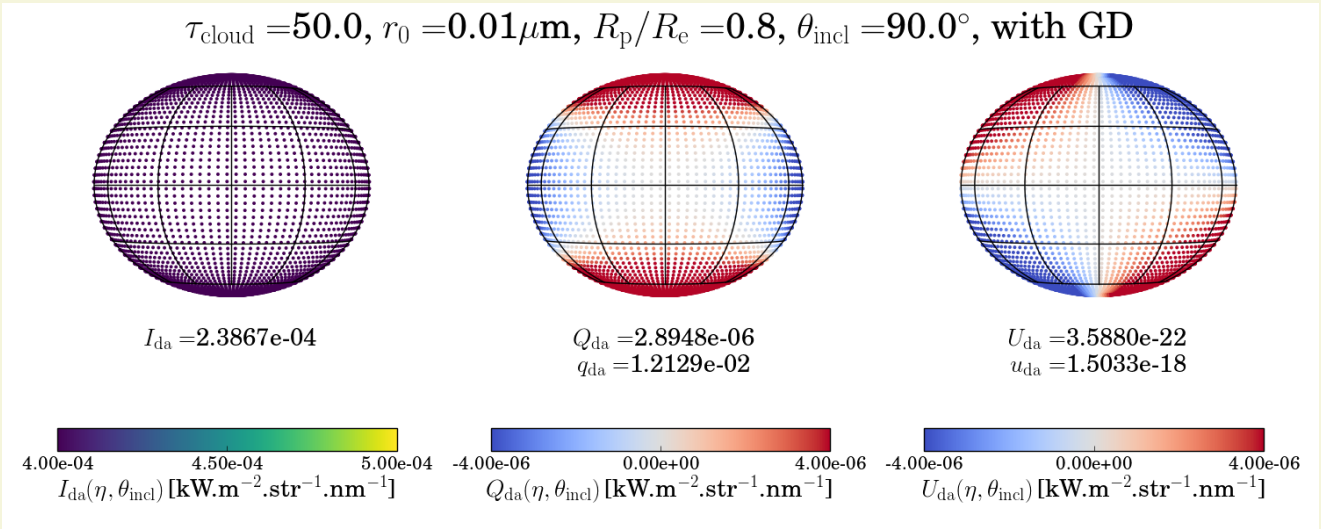

Effect of oblateness and inclination angle

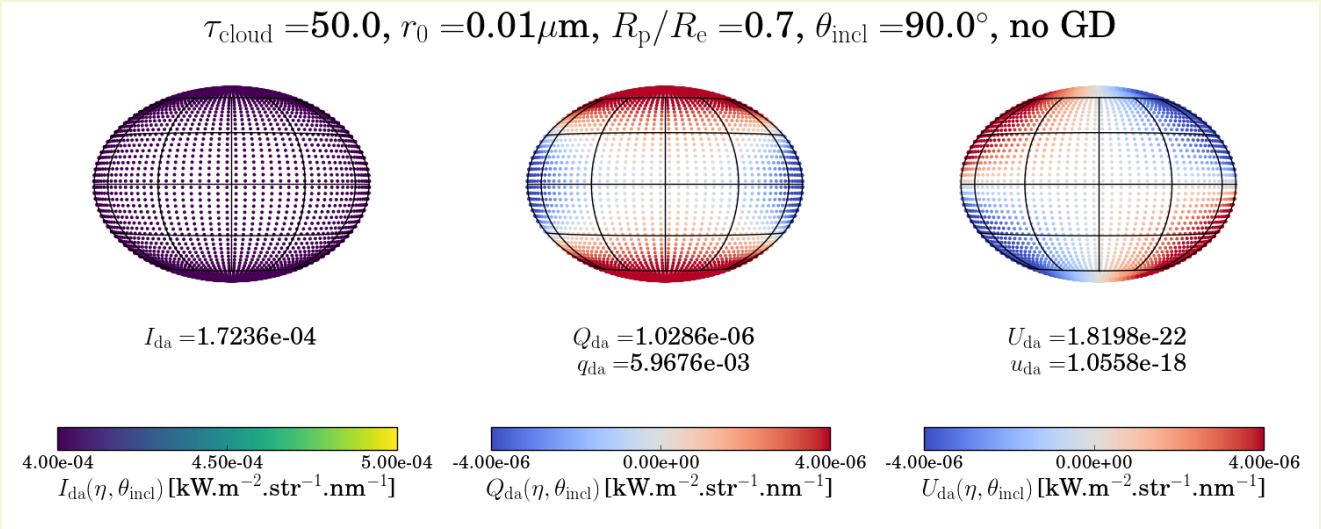

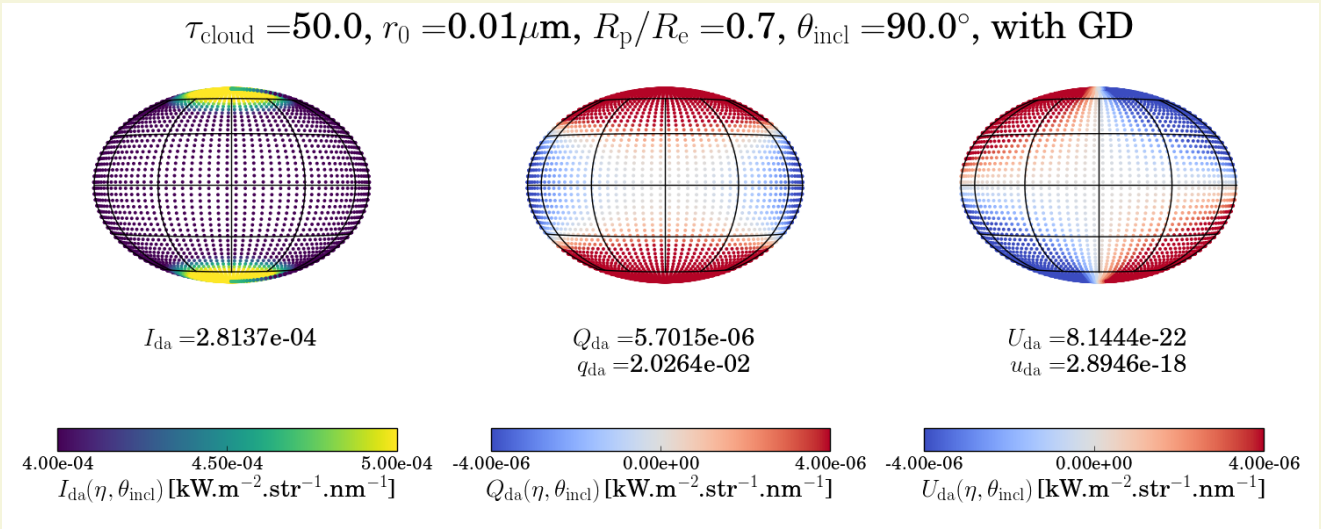

Effect of oblateness and inclination angle

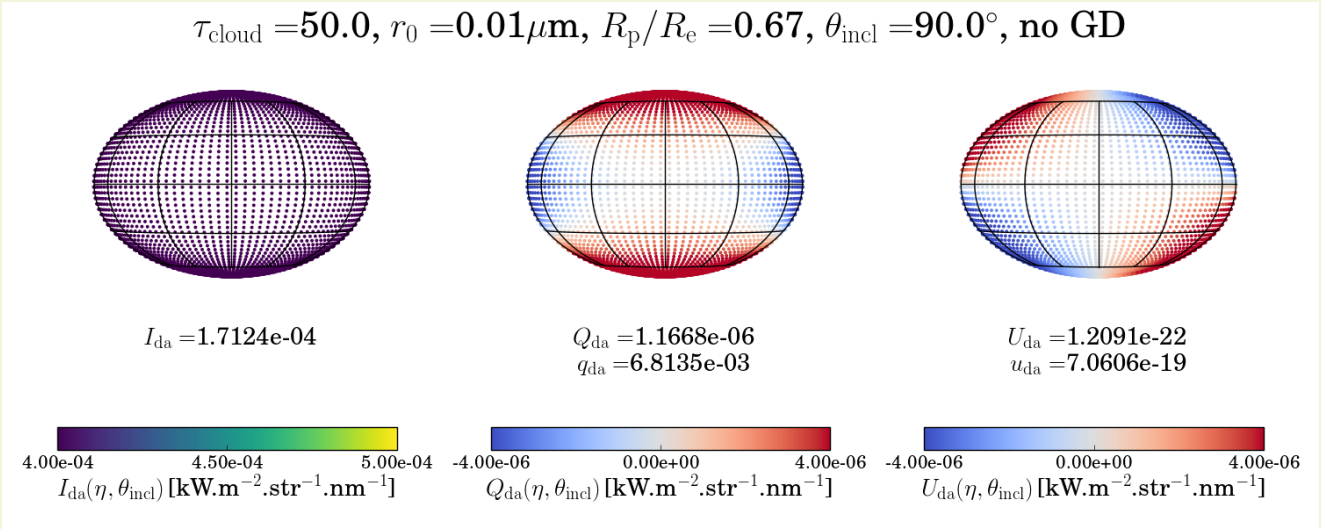

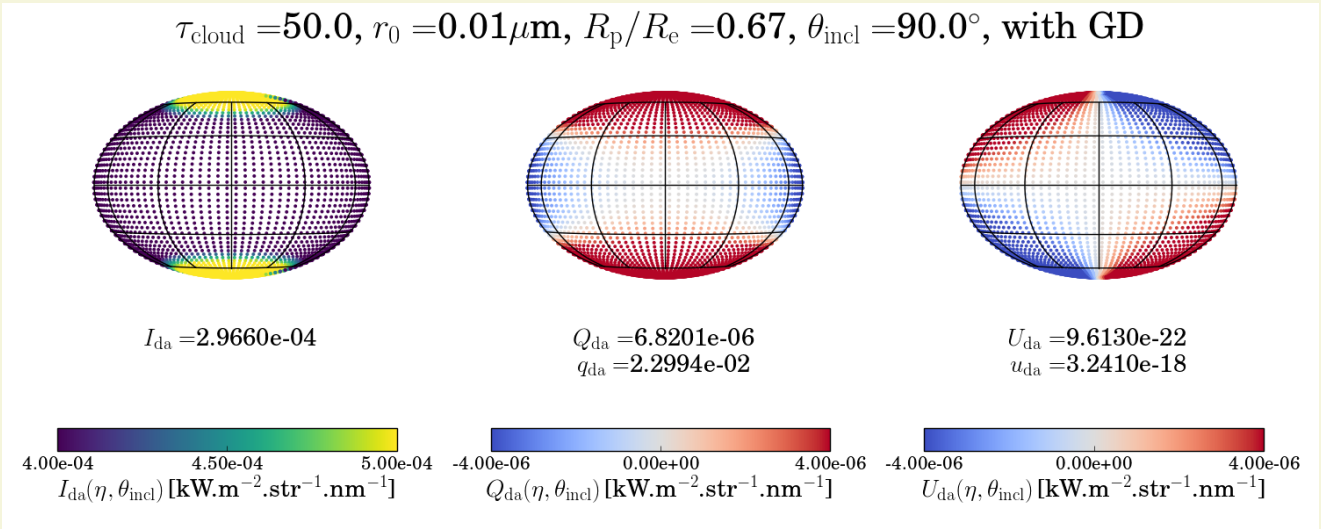

Effect of oblateness and inclination angle

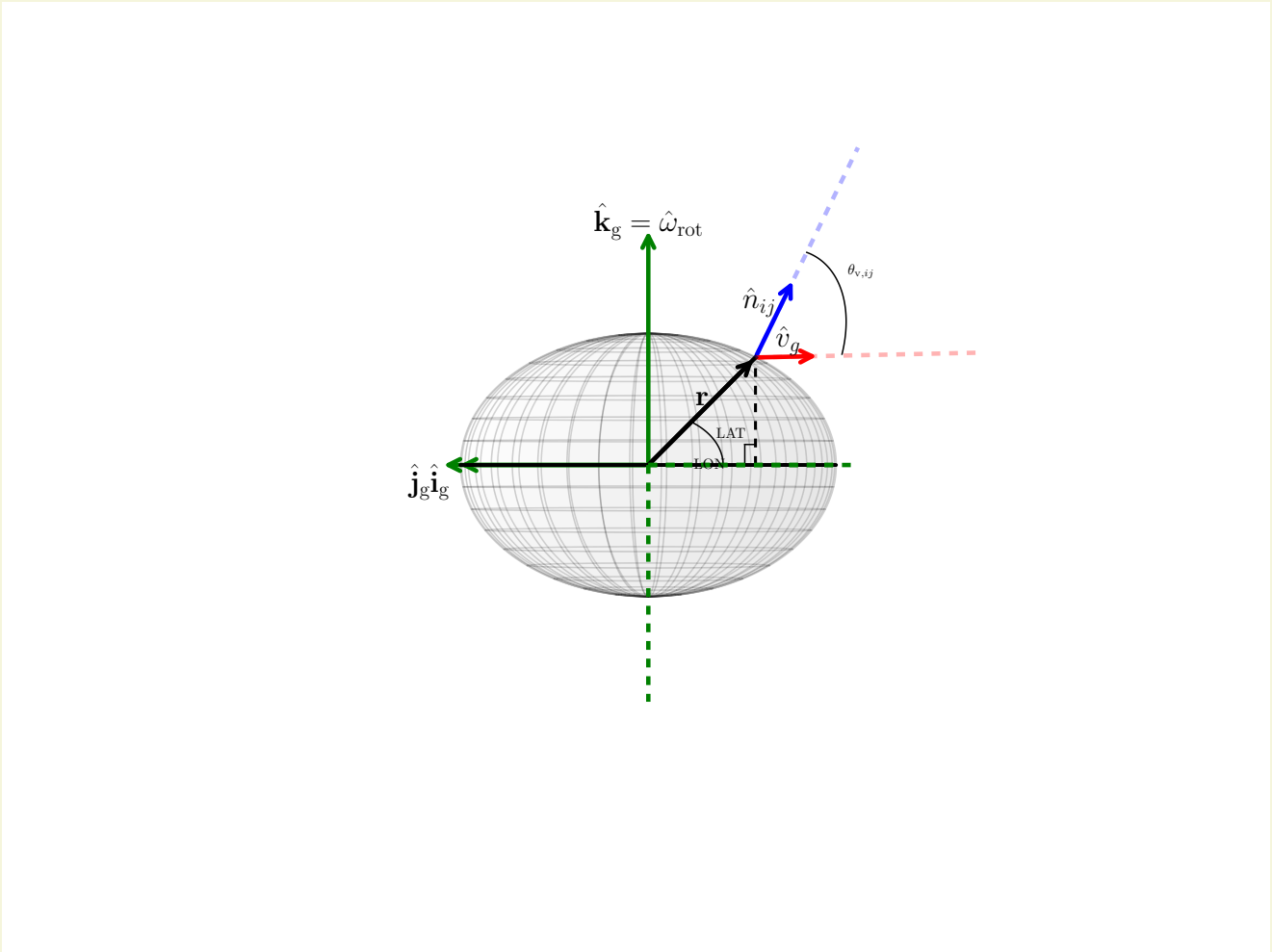

- The inclination angle, $\theta_{\rm incl}$, now plays a role in determining the angles at which different facets of the BD surface are oriented with respect to the viewing plane

Effect of oblateness and inclination angle

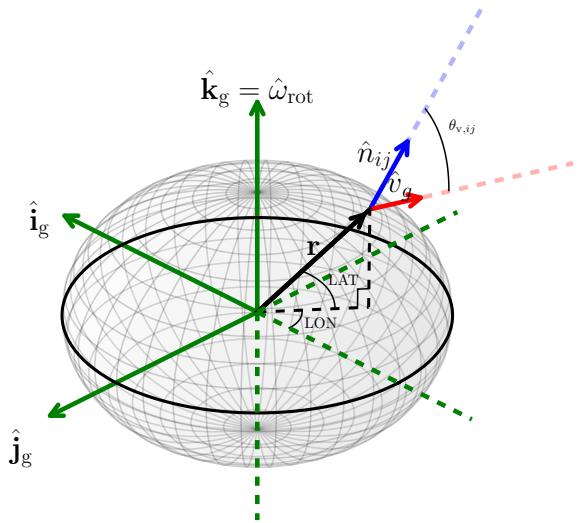

- The inclination angle, $\theta_{\rm incl}$, now plays a role in determining the angles at which different facets of the BD surface are oriented with respect to the viewing plane

Effect of oblateness and inclination angle

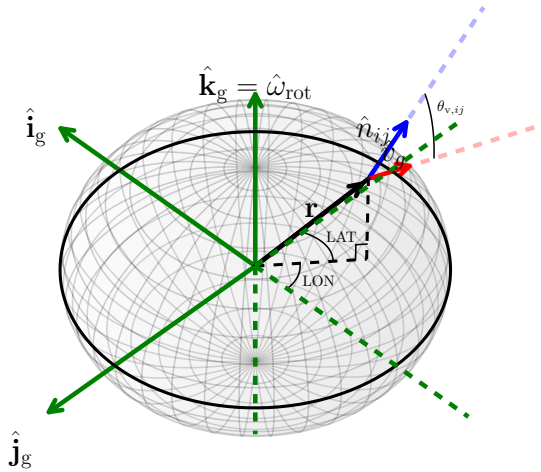

- The inclination angle, $\theta_{\rm incl}$, now plays a role in determining the angles at which different facets of the BD surface are oriented with respect to the viewing plane

Effect of oblateness and inclination angle

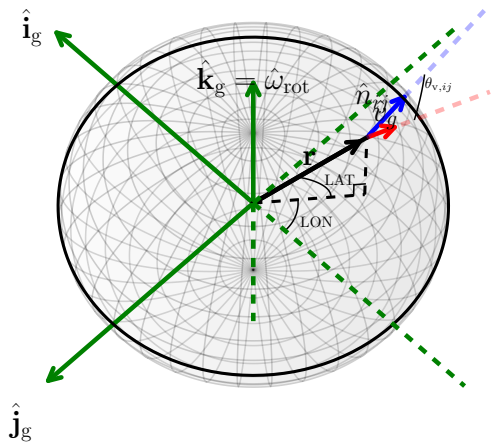

- The inclination angle, $\theta_{\rm incl}$, now plays a role in determining the angles at which different facets of the BD surface are oriented with respect to the viewing plane

Effect of oblateness and inclination angle

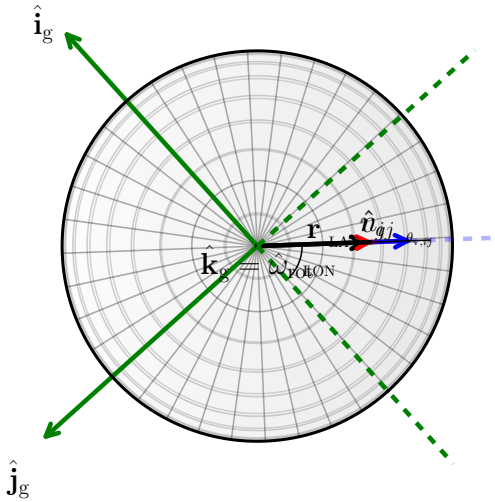

- The inclination angle, θ_{incl}, now plays a role in determining the angles at which different facets of the BD surface are oriented with respect to the viewing plane

Effect of oblateness and inclination angle

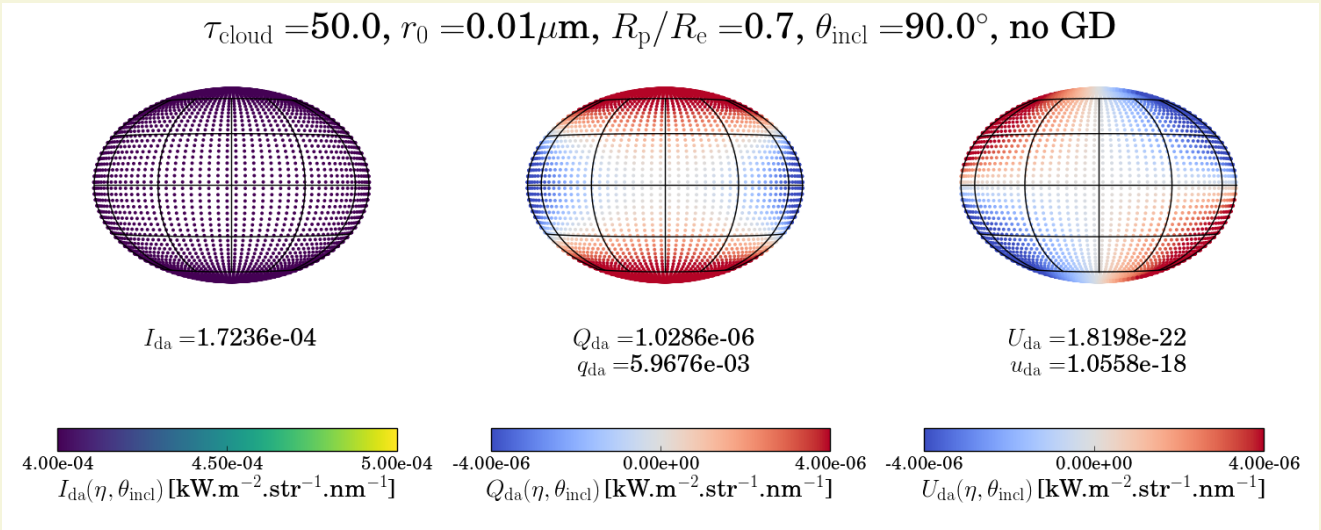

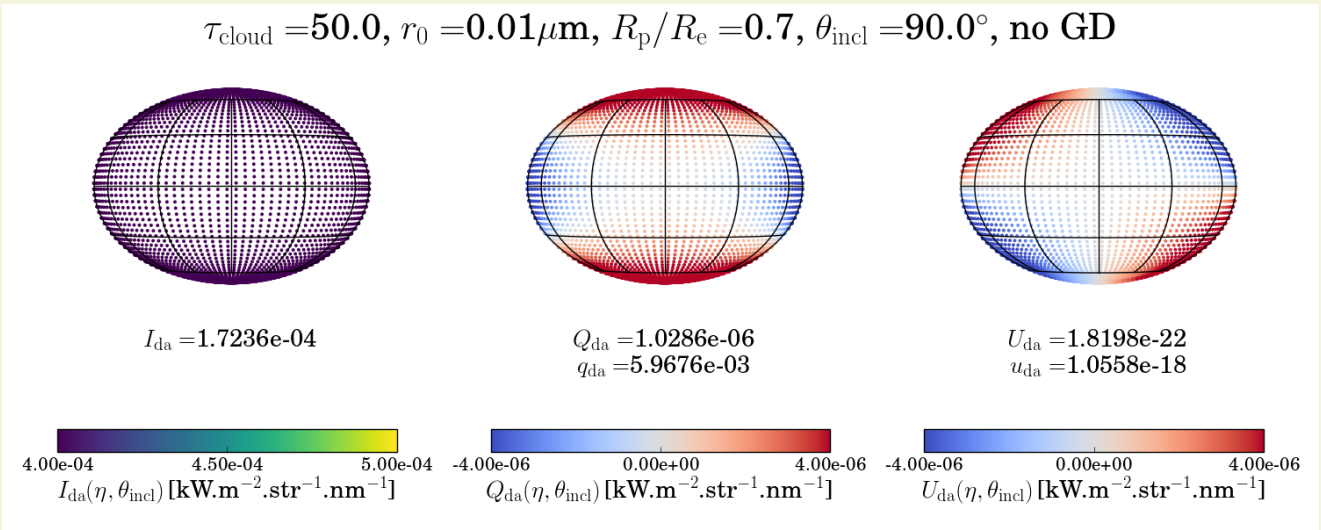

Effect of oblateness and inclination angle

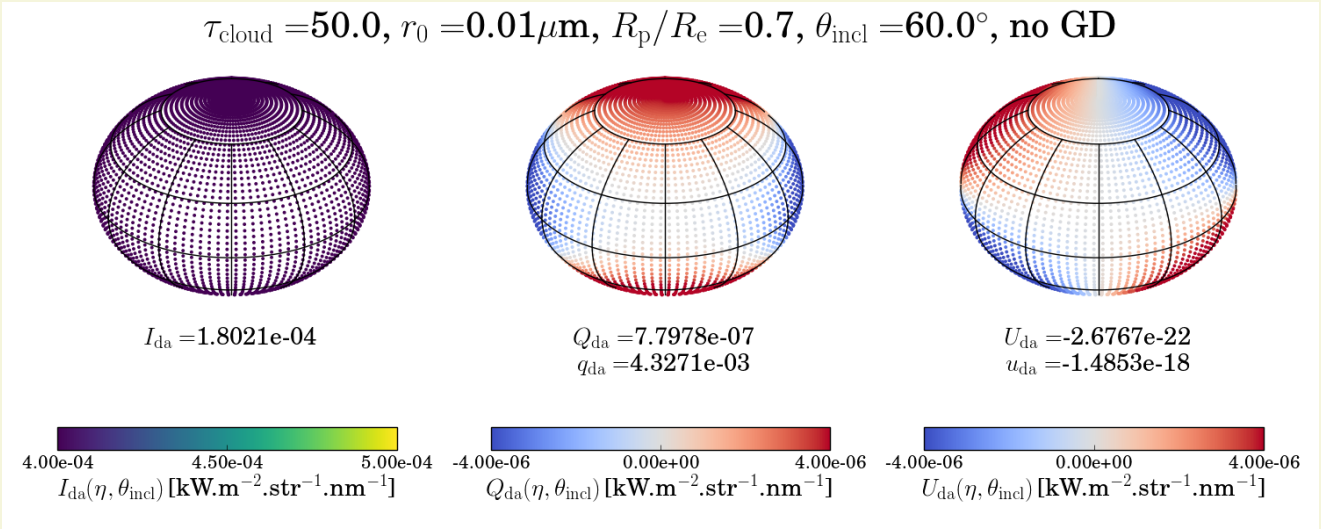

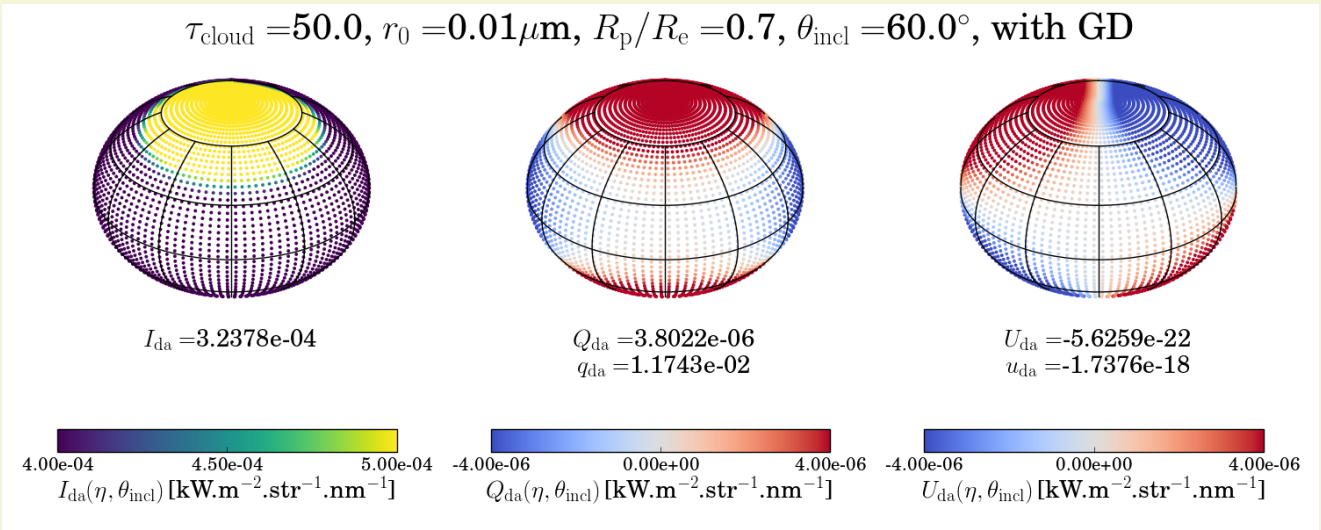

Effect of oblateness and inclination angle

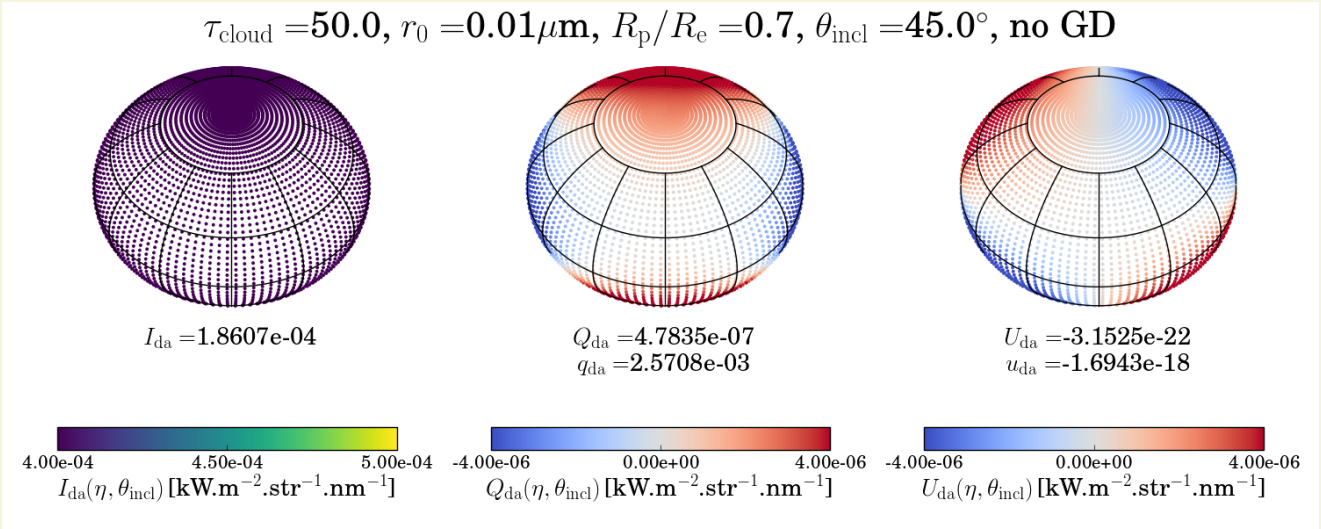

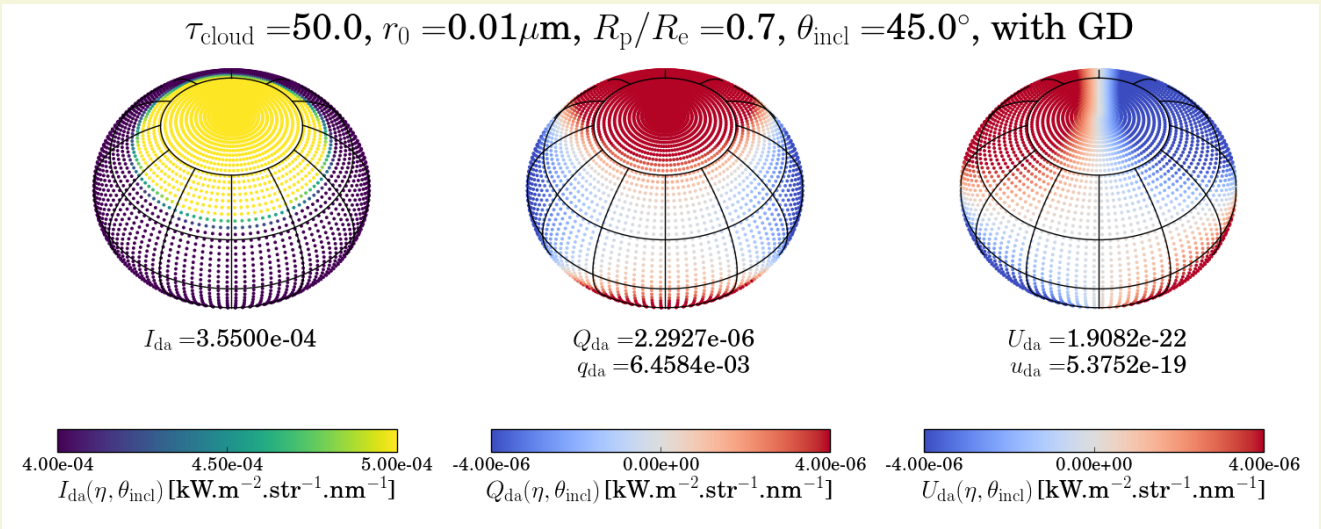

Effect of oblateness and inclination angle

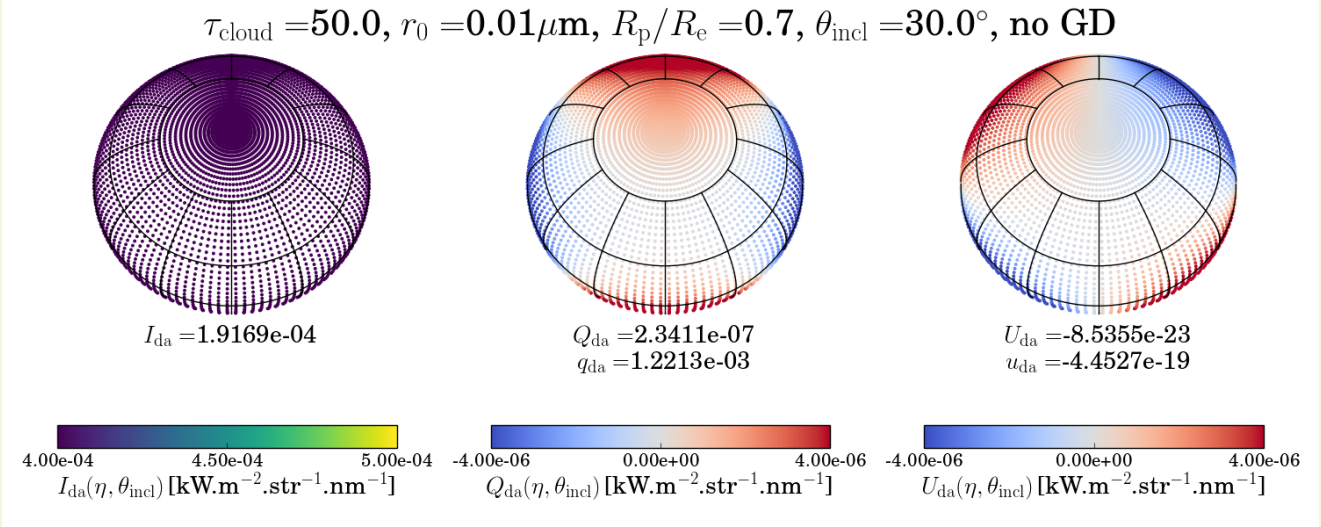

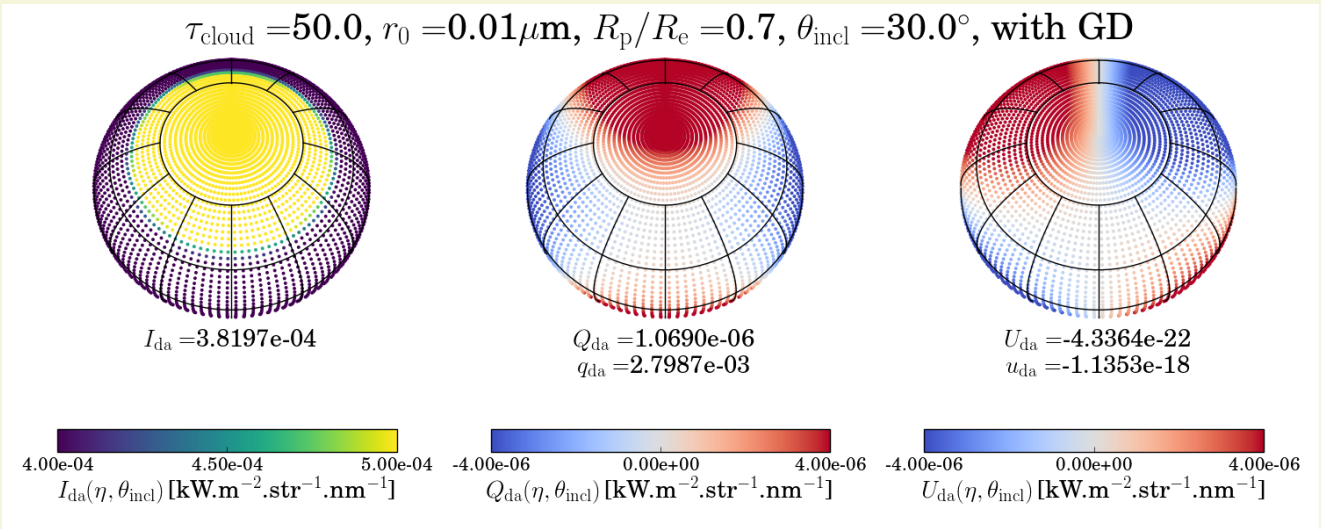

Effect of oblateness and inclination angle

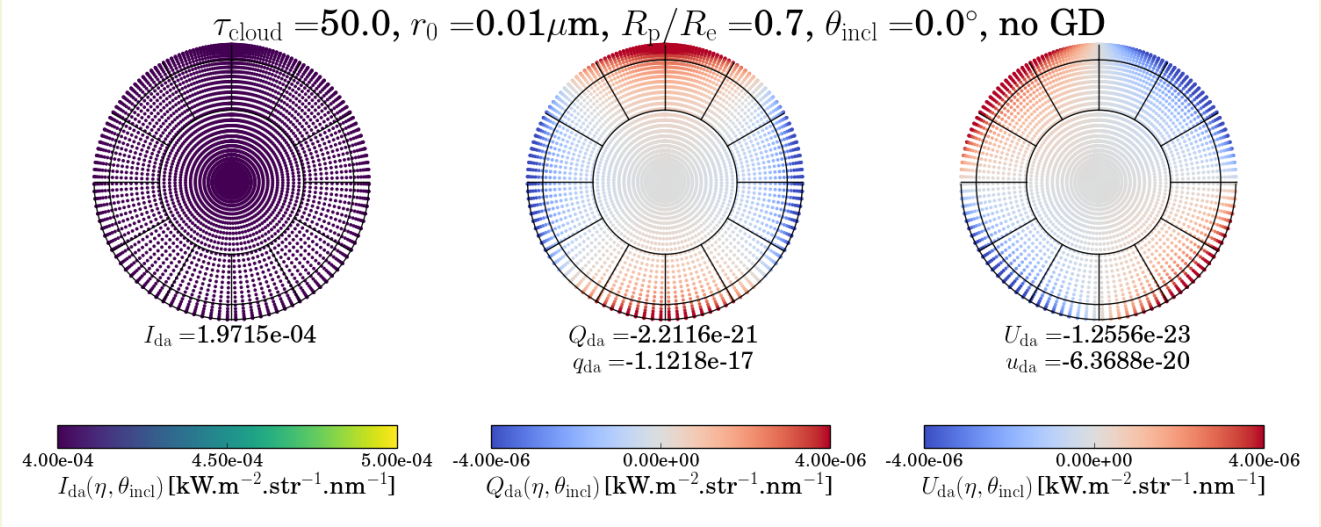

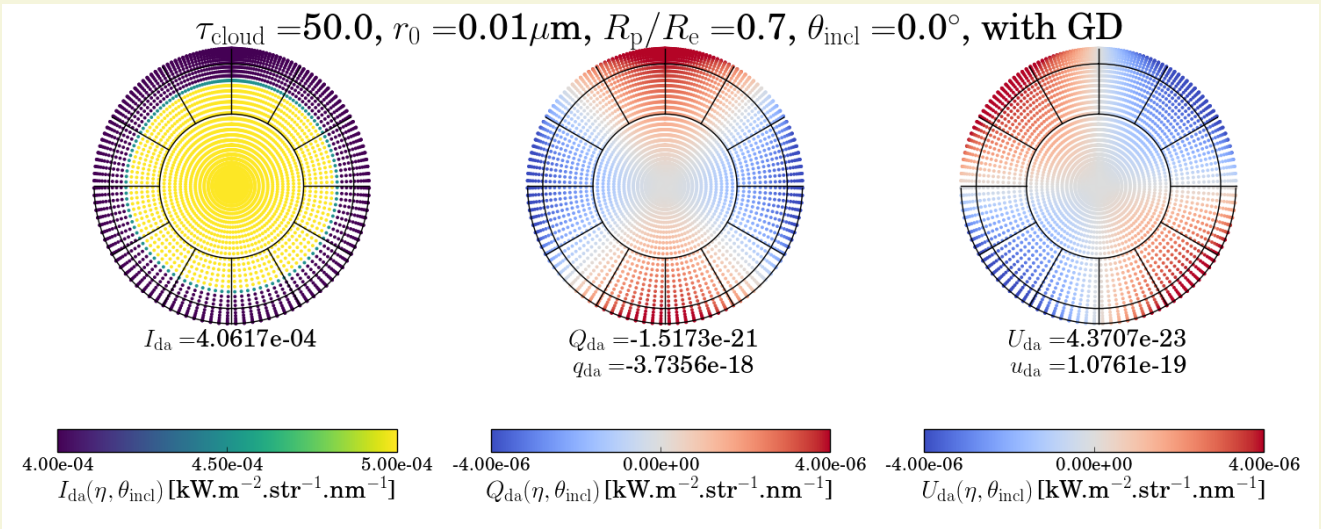

Effect of oblateness and inclination angle

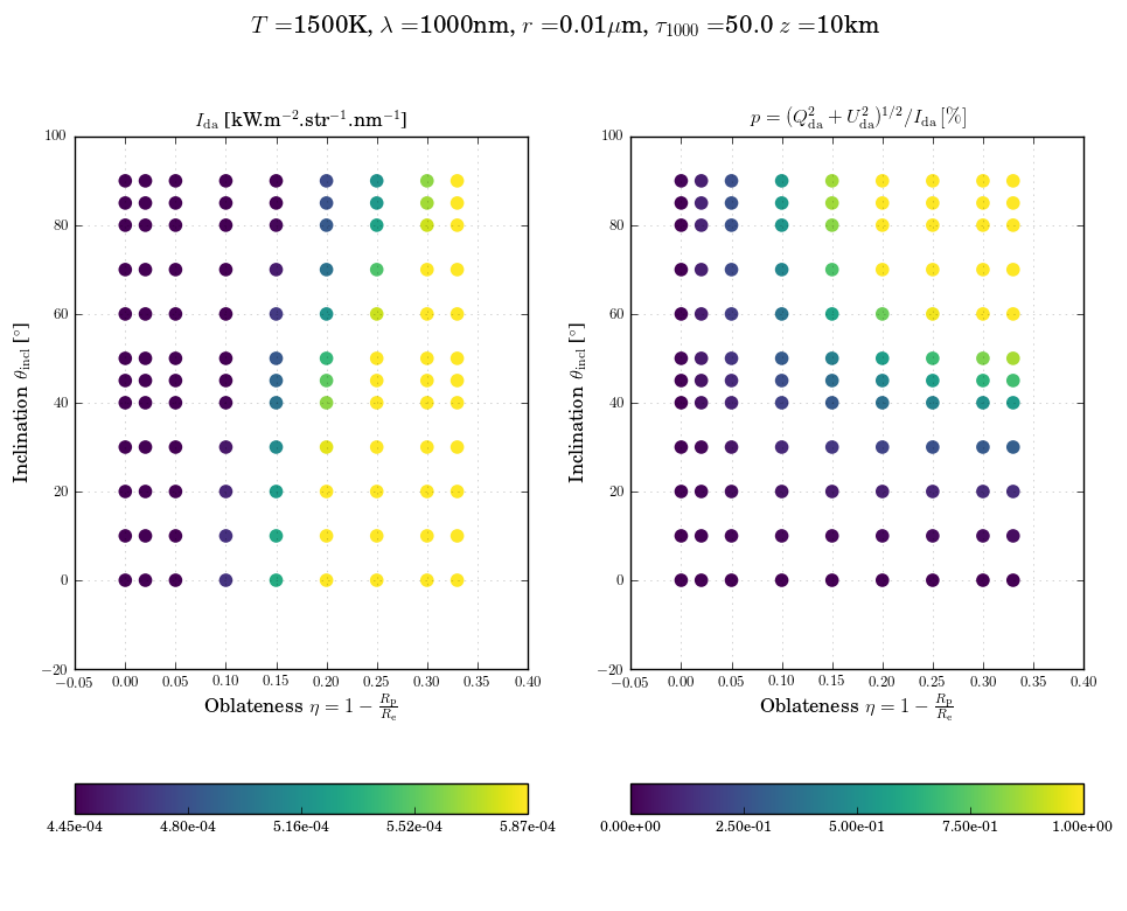

- Both intensity and polarization are functions of obalteness, η, and inclination angle, $\theta_{\rm incl}$

Effect of oblateness and inclination angle

- The angle of polarization, α_0, is obtained by rotating the viewing plane until $U_{\rm da} = 0$
- If inclination angle, $\theta_{\rm incl}$, can also be determined from $I_{\rm da}$ and $p_{\rm da}$, the combined knowledge of α_0 and $\theta_{\rm incl}$ would provide the exact spatial orientation of the axis of the BD

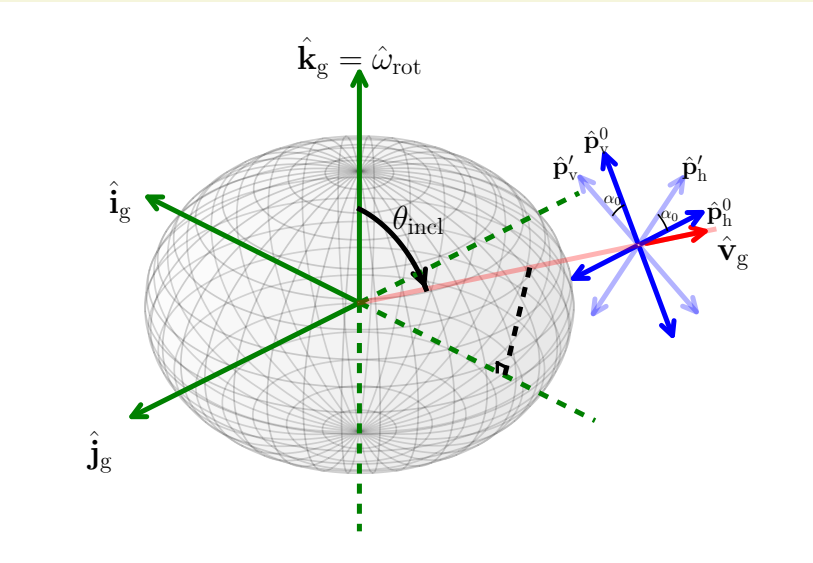

Gravitational darkening

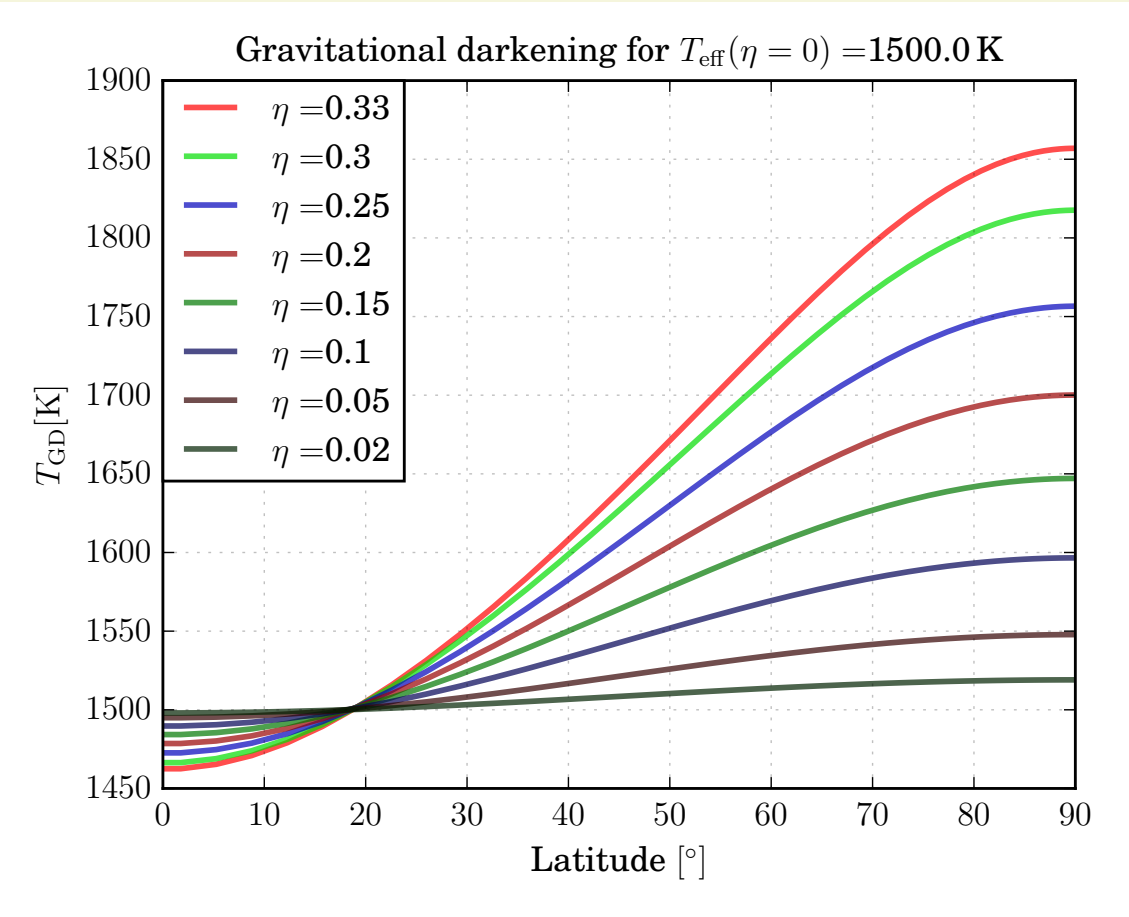

Gravitational darkening

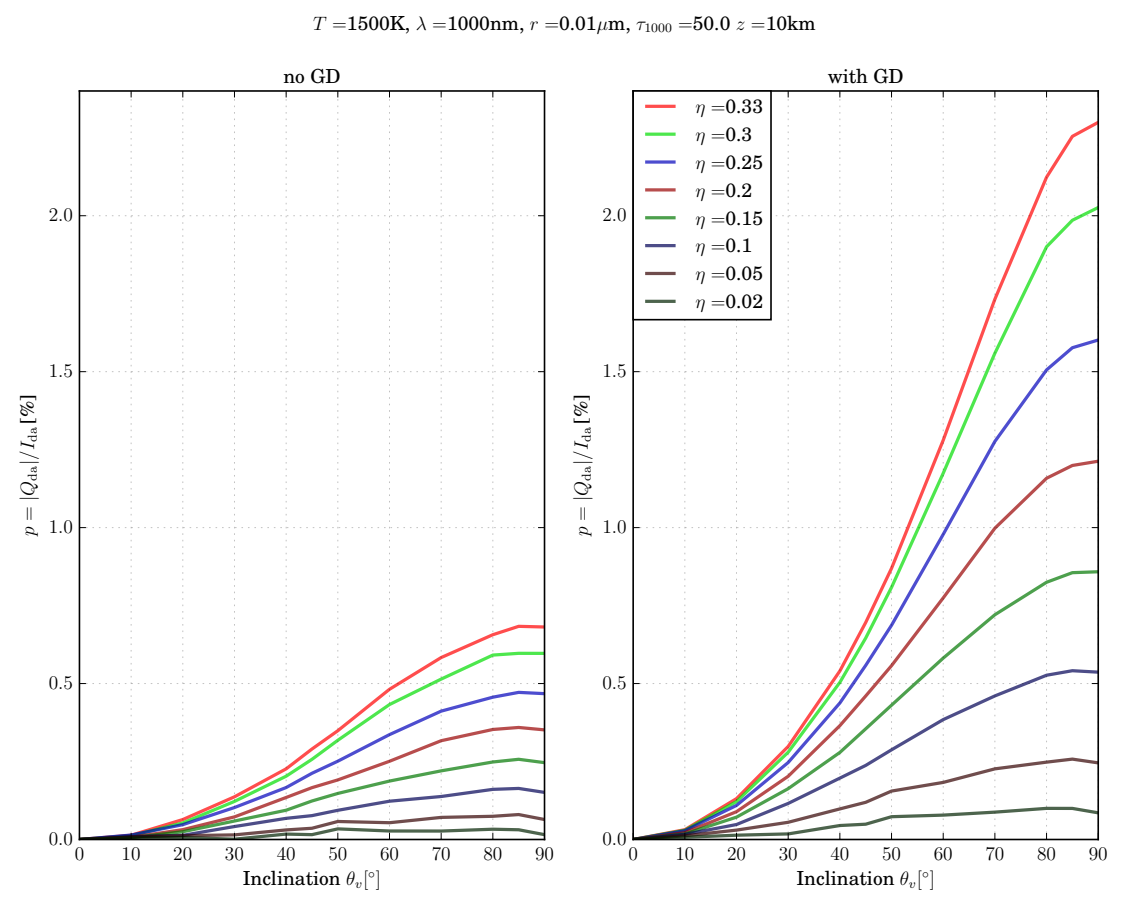

Effects of cloud properties: optical thickness, cloud grain size

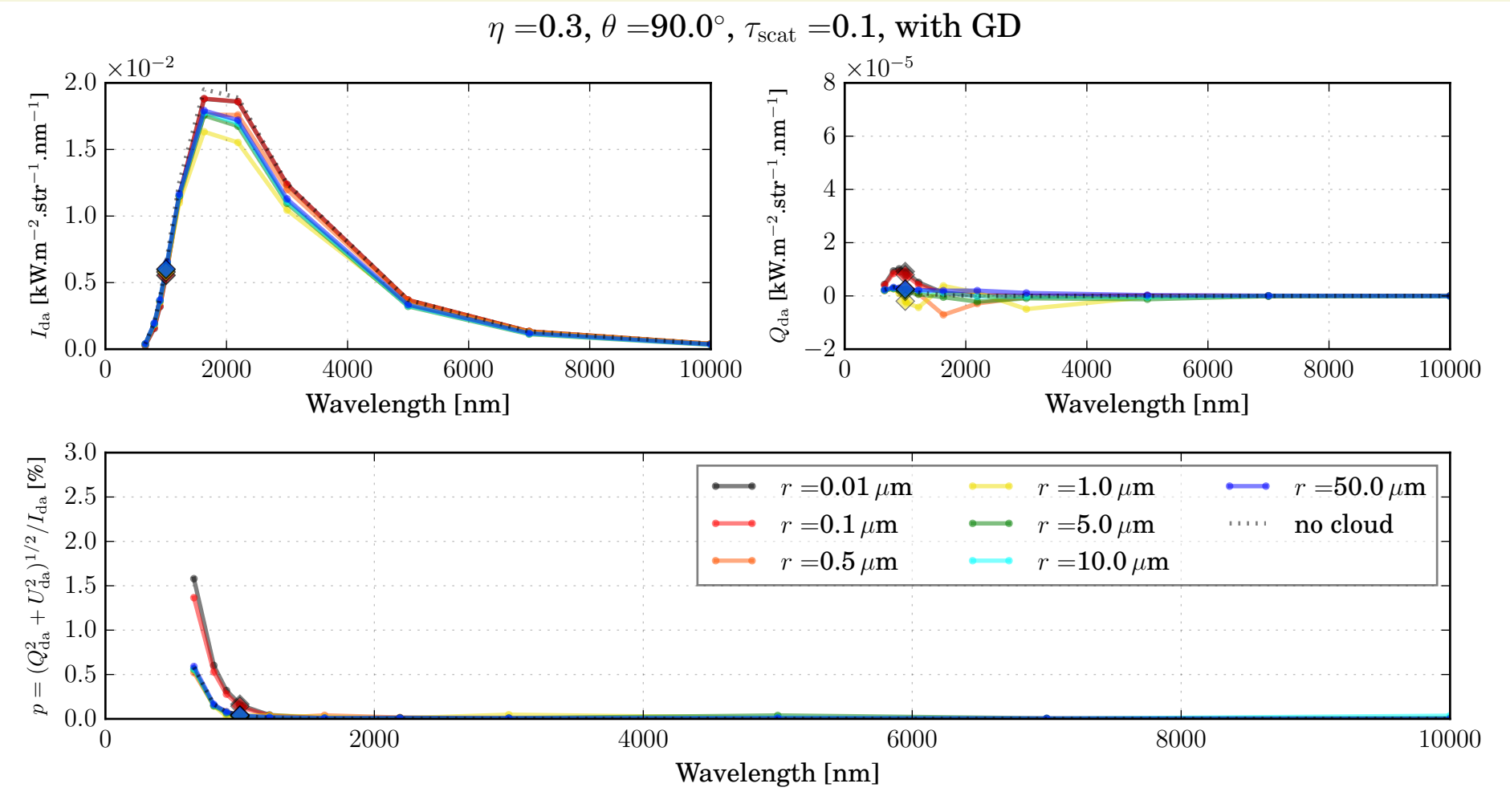

Effects of cloud properties: optical thickness, cloud grain size

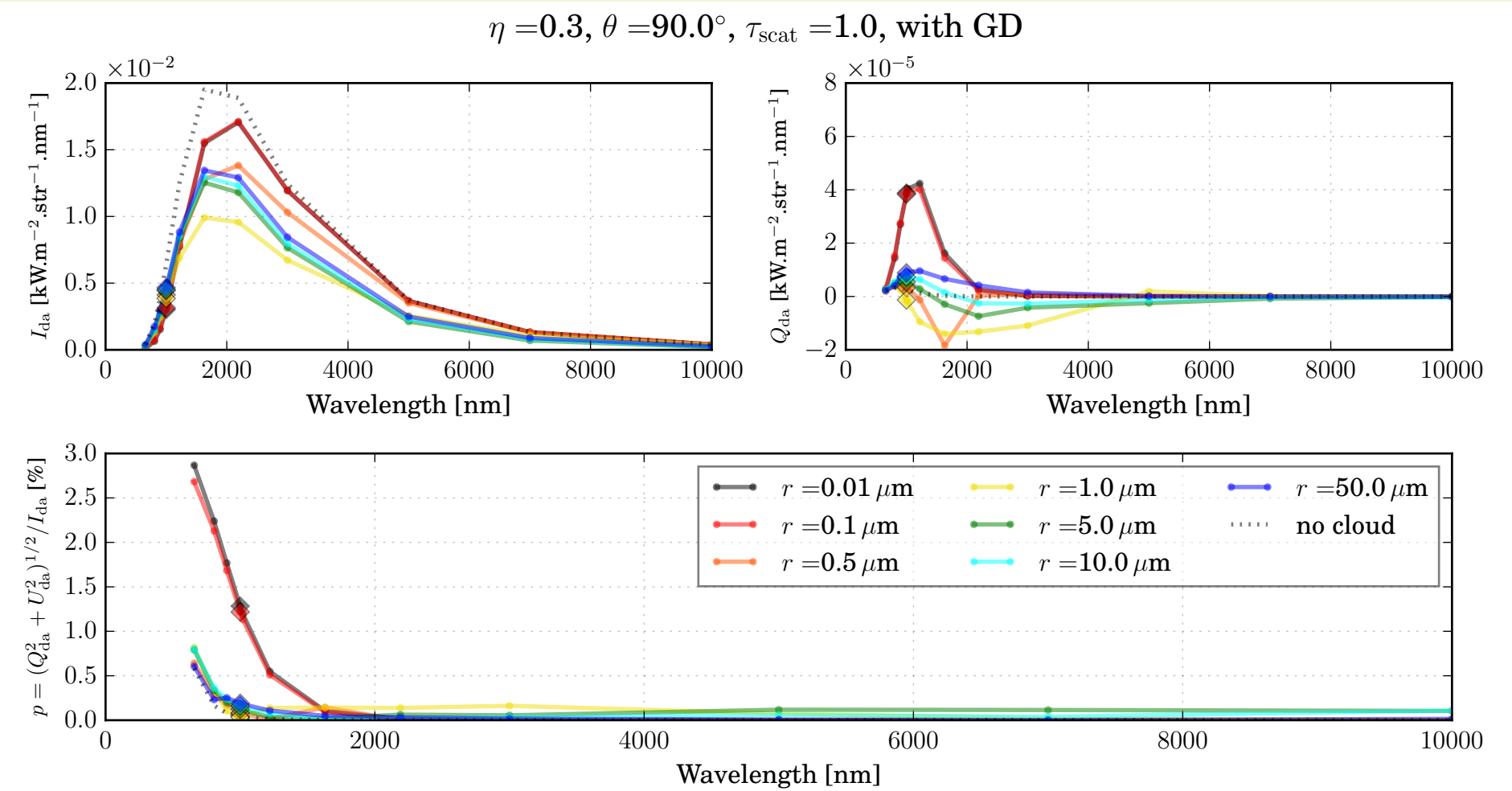

Effects of cloud properties: optical thickness, cloud grain size

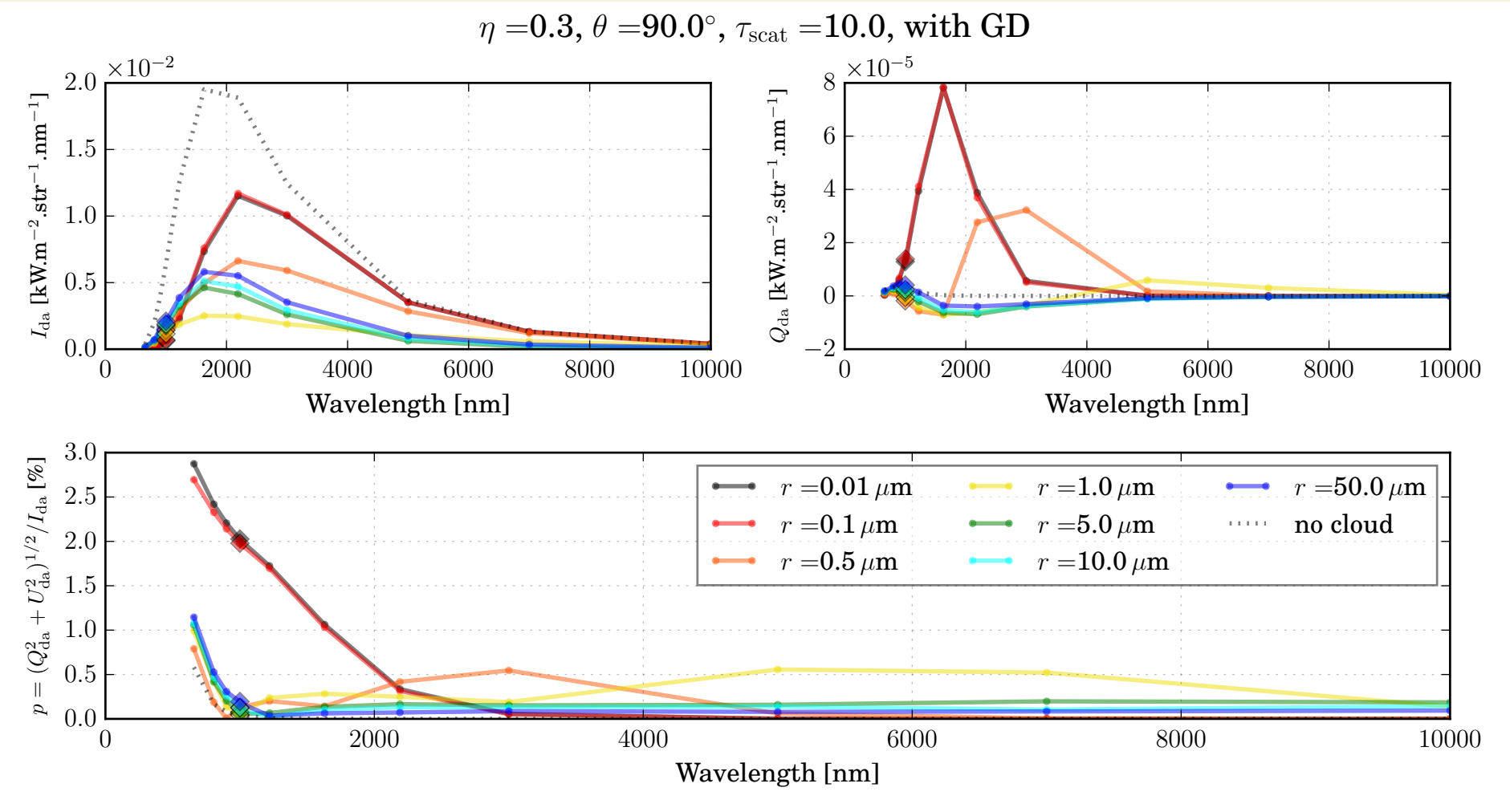

Photometry: Need for detailed consideration of opacity

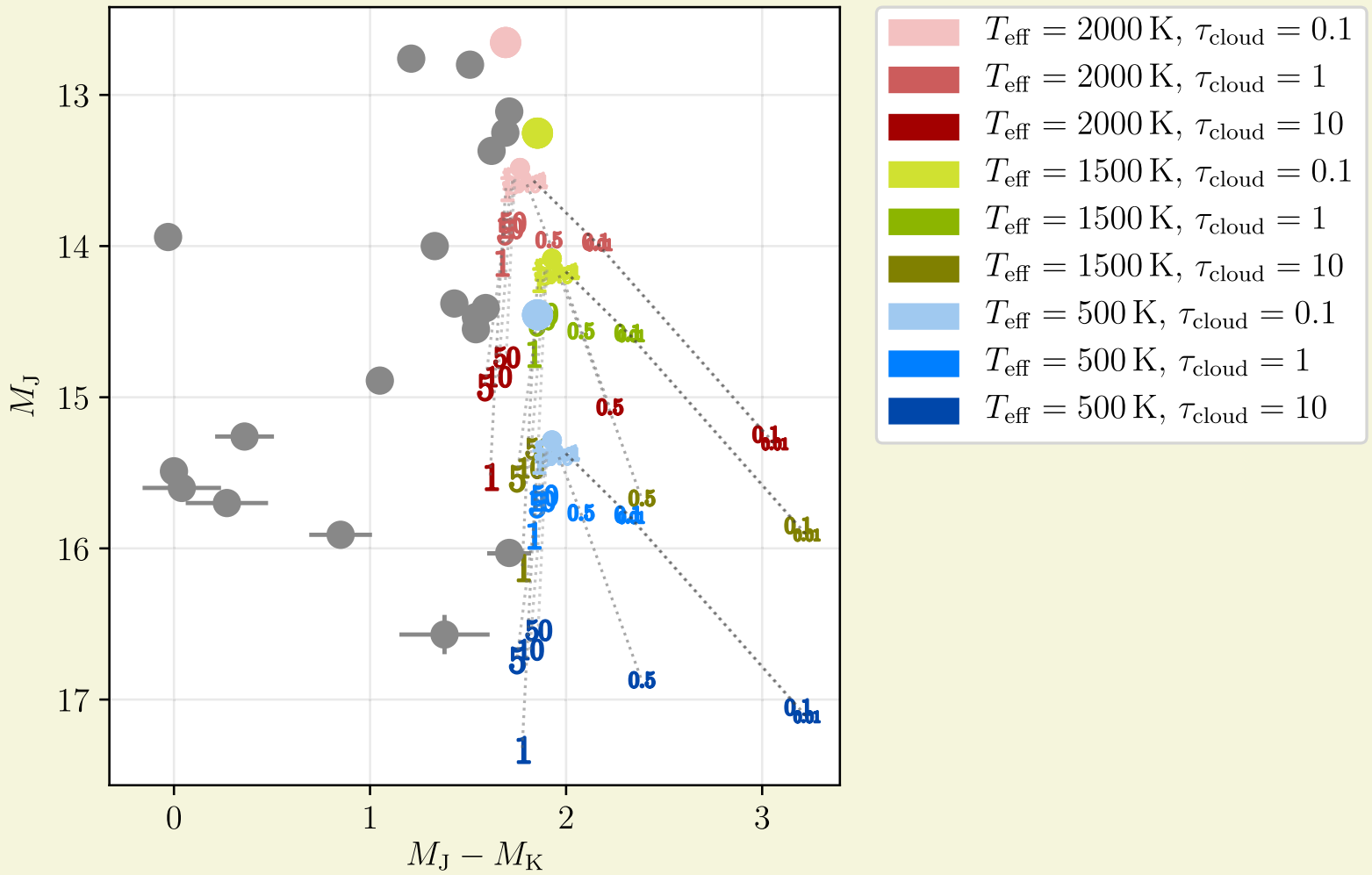

(Grey circles represent observed BDs from Burgasser (2007))

Molecular opacities

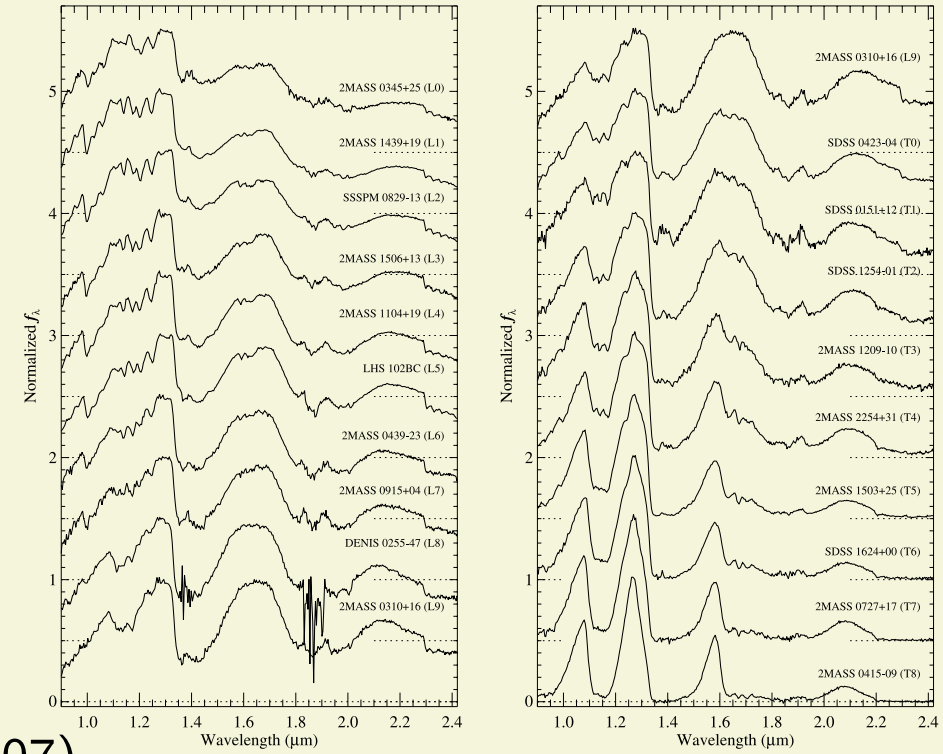

(Burgasser et al. 2007)

- L-dwarfs are only affected by weak absorption due to H_2O in the NIR, while the deeper atmospheric column of T-dwarfs feature strong pressure-broadened alkali lines in the optical, near-saturation CH_4 absorption in the NIR, and H_2 CIA near the K-band.

Polarimetry: Effect of clouds

Photosphere at BOA, $T_{\rm eff} = 2000\,$K, no GD

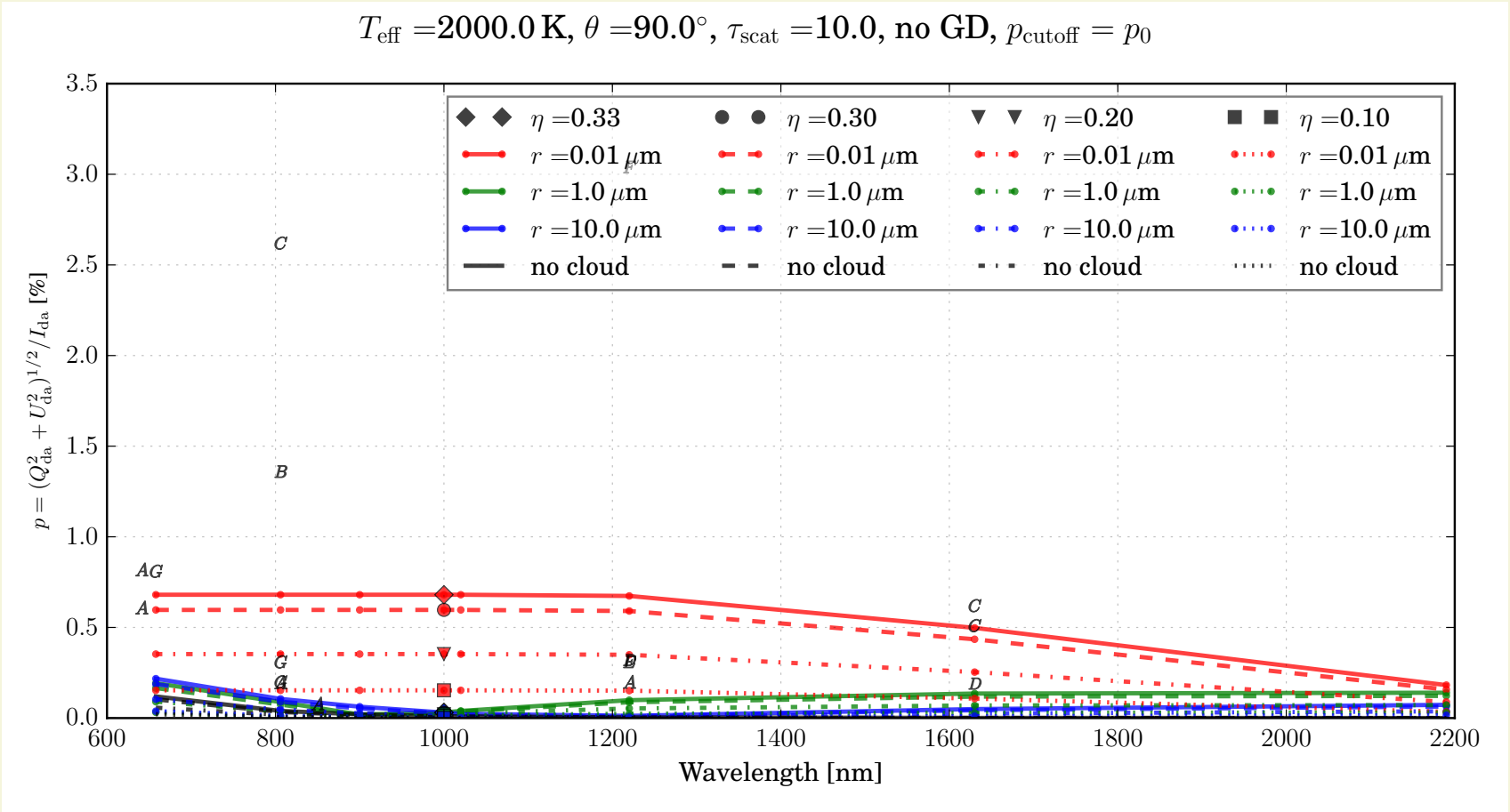

Polarimetry: Effect of clouds

Photosphere at BOA, $T_{\rm eff} = 2000\,{\rm K}$, with GD

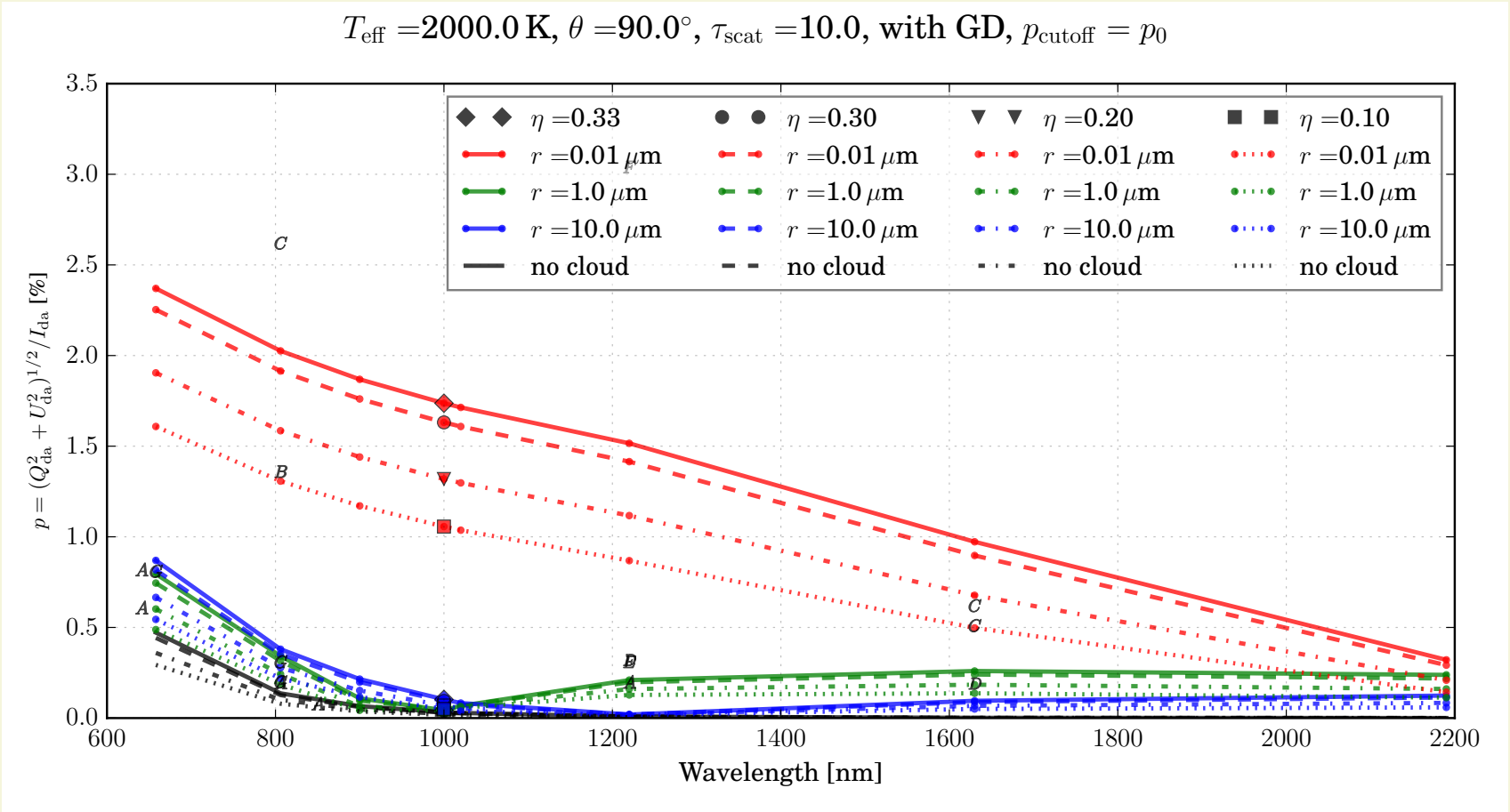

Polarimetry: Effect of clouds

Photosphere at BOA, $T_{\rm eff} = 1500\,$K, no GD

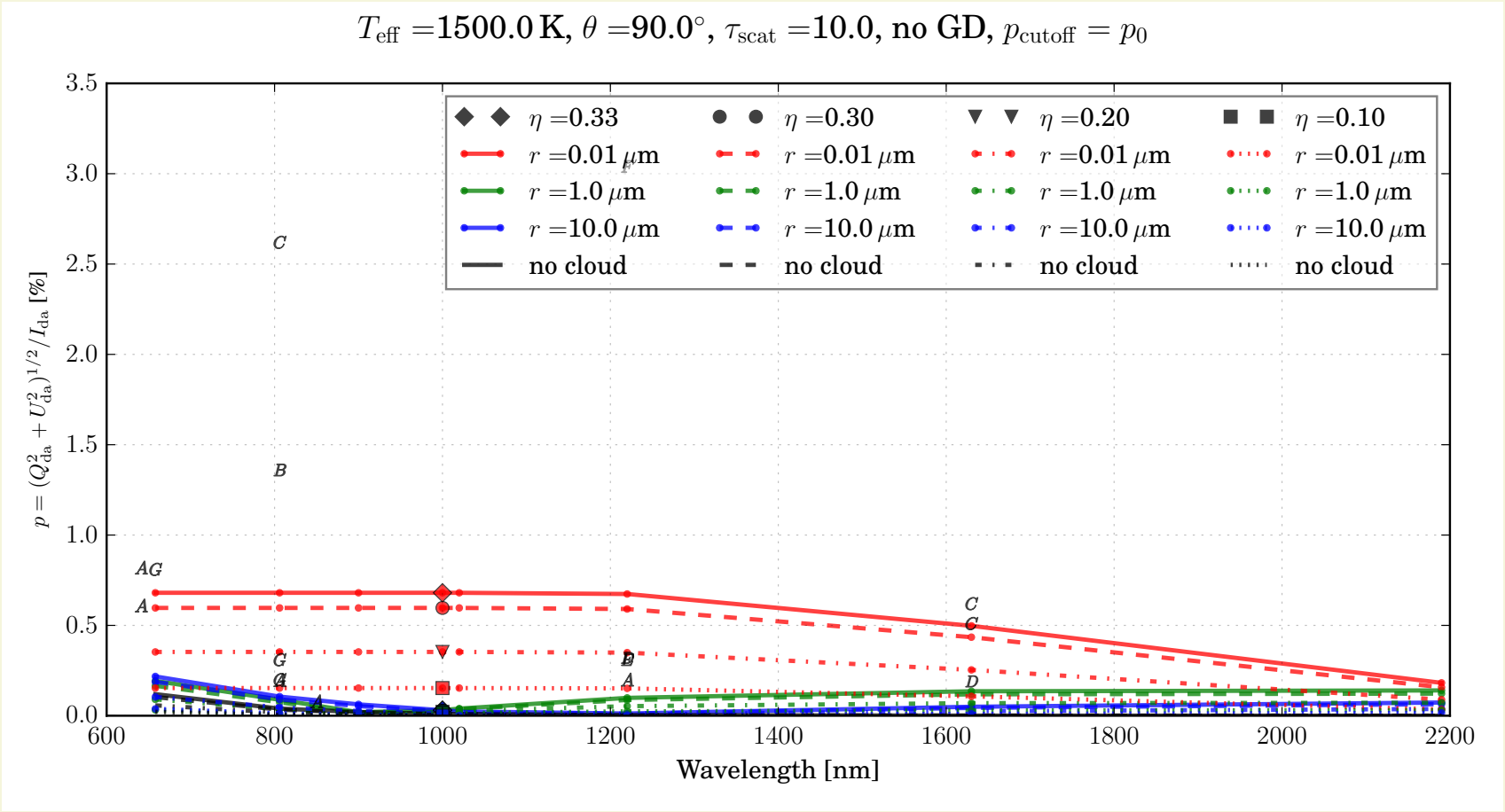

Polarimetry: Effect of clouds

Photosphere at BOA, $T_{\rm eff} = 1500\,{\rm K}$, with GD

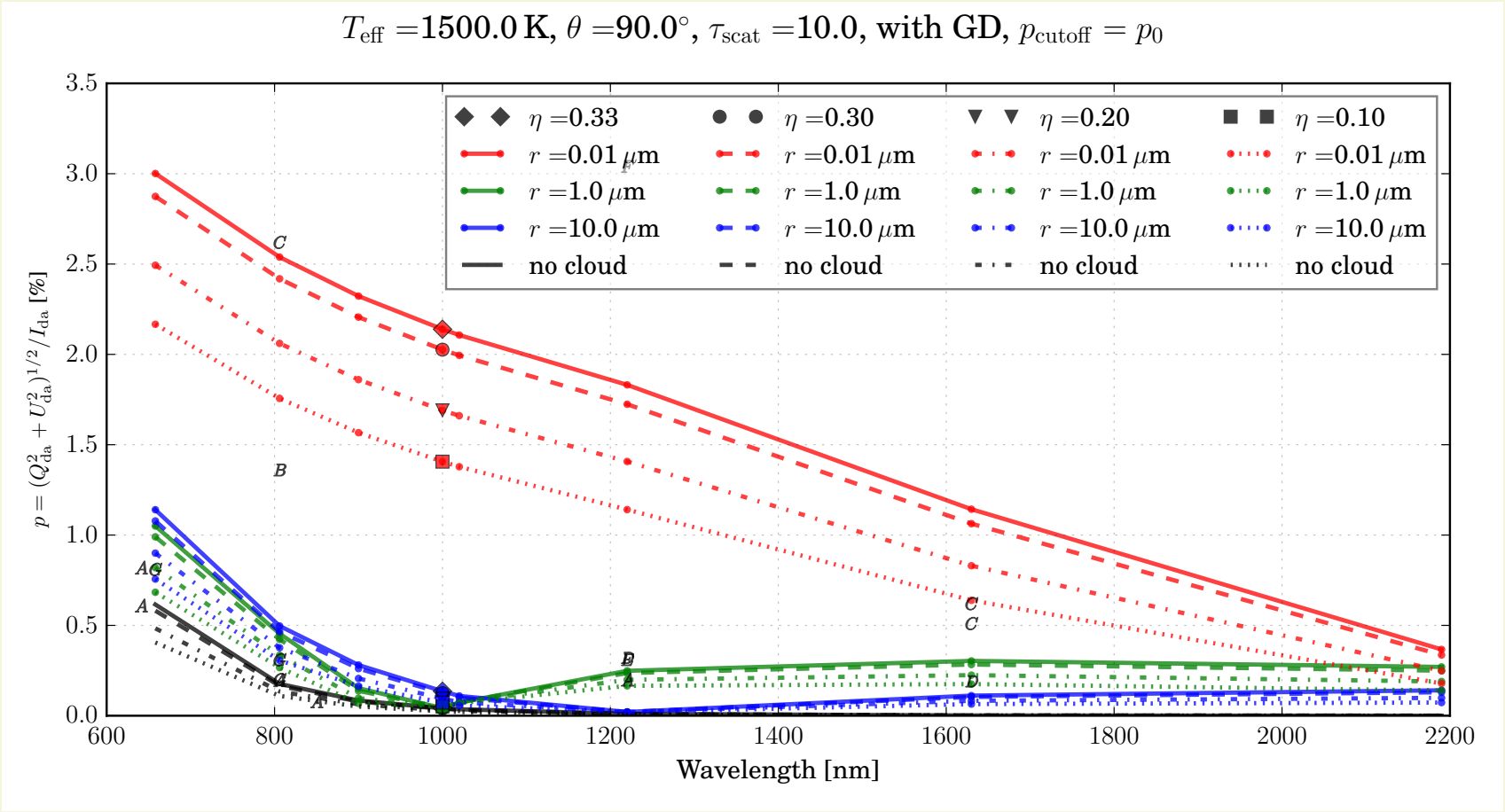

Polarimetry: Effect of clouds

Photosphere at BOA, $T_{\rm eff} = 500\,{\rm K}$, no GD

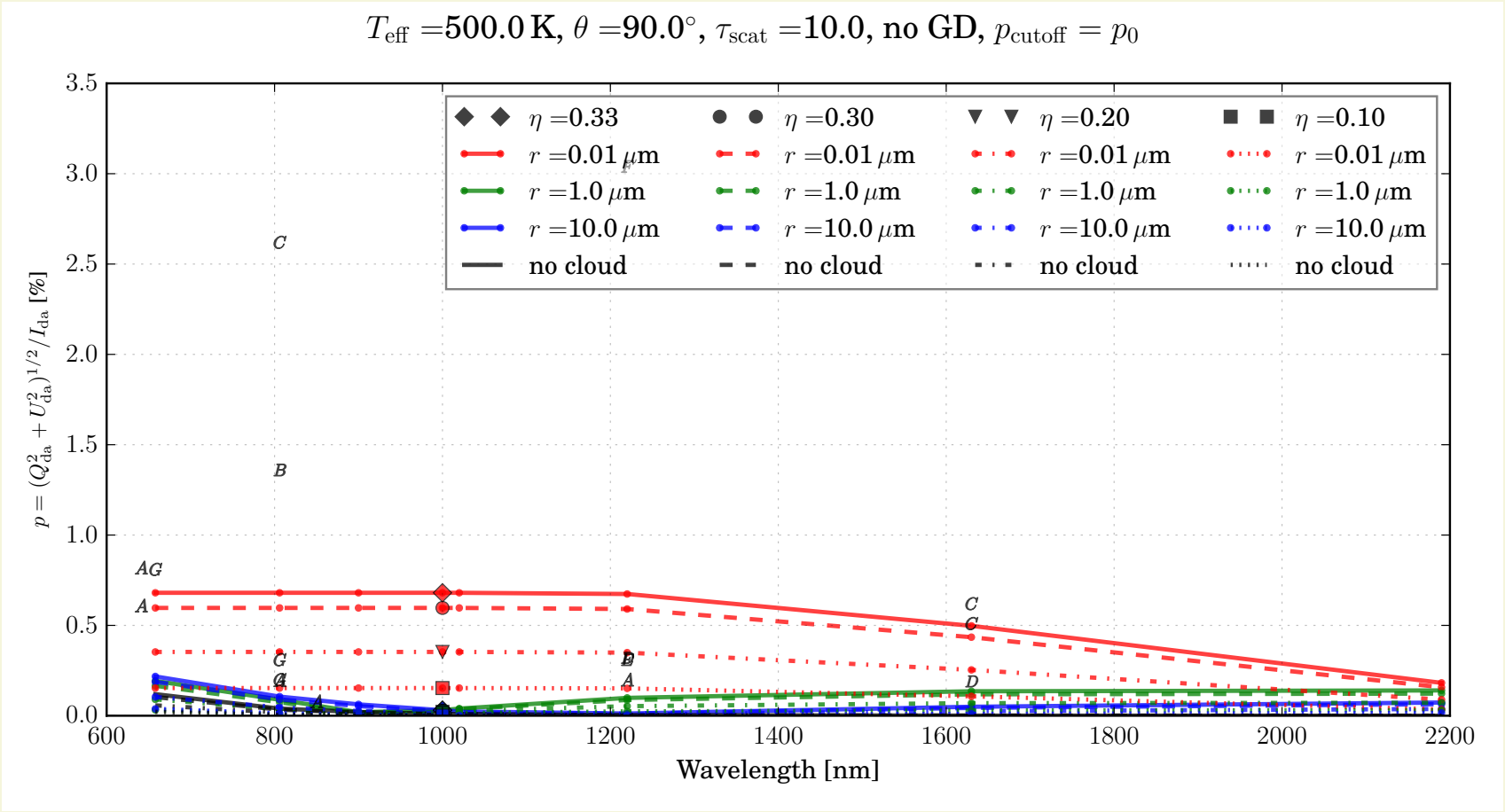

Polarimetry: Effect of clouds

Photosphere at BOA, $T_{\rm eff} = 500\,{\rm K}$, with GD

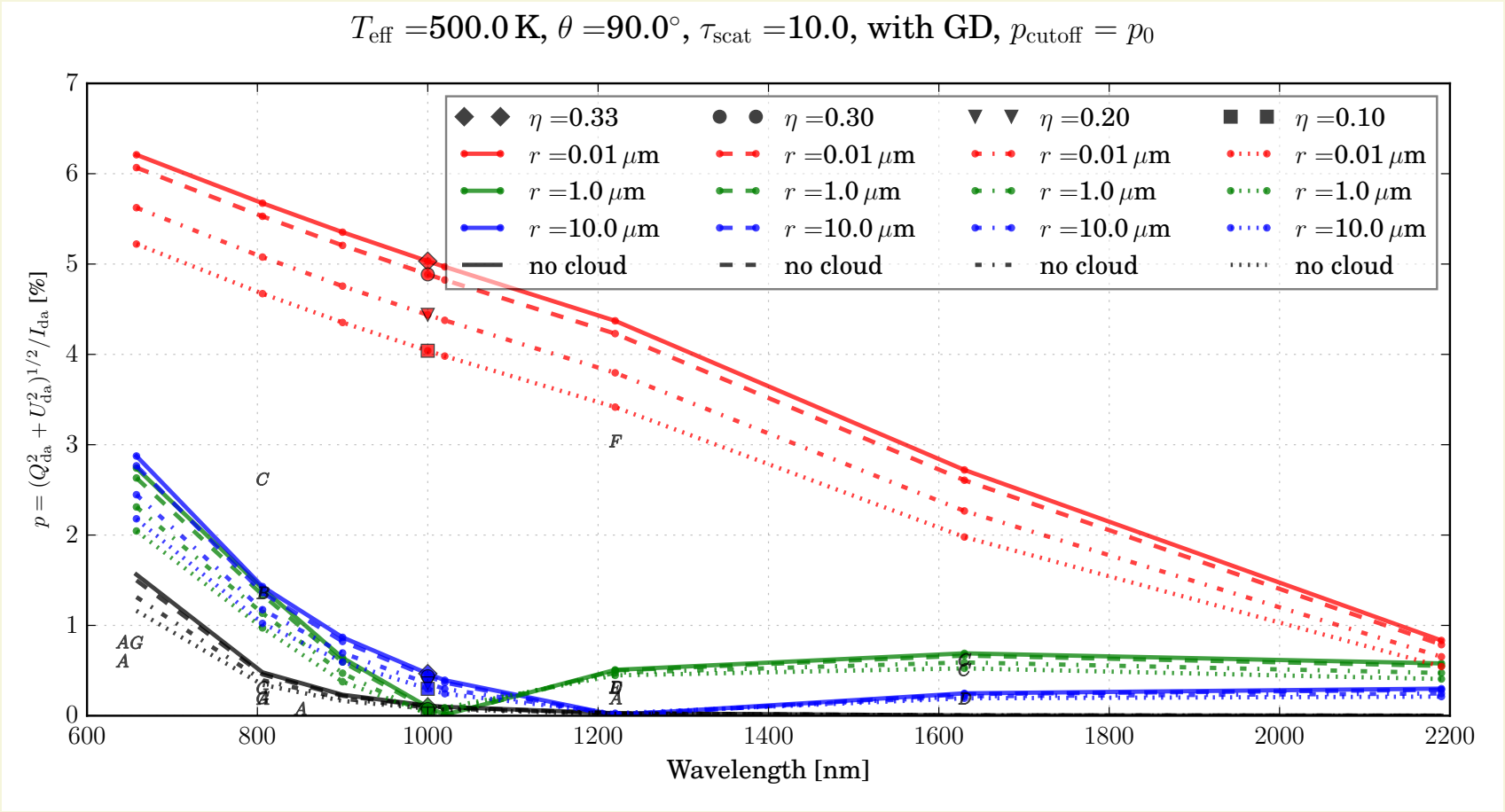

Preliminary interpretation of polarimetric observations

- Comparisons with 7 BD observations for which polarimetric measurements were available
- Most cases had intermediate values that would require more sophisticated retrieval methods to fit (subject to constraints available)
- 2MASS J2244 (L6.5, $p_{\rm da} = (2.5 \pm 0.5)\%$ in the I-band), however, is an extreme case that could only be simulated if:

Preliminary interpretation of polarimetric observations

- Comparisons with 7 BD observations for which polarimetric measurements were available
- Most cases had intermediate values that would require more sophisticated retrieval methods to fit (subject to constraints available)
- 2MASS J2244 (L6.5, $p_{\rm da} = (2.5 \pm 0.5)\%$ in the I-band), however, is an extreme case that could only be simulated if:
  1. $T_{\rm eff}$ was less than $\sim 1500\,{\rm K}$.

Preliminary interpretation of polarimetric observations

- Comparisons with 7 BD observations for which polarimetric measurements were available
- Most cases had intermediate values that would require more sophisticated retrieval methods to fit (subject to constraints available)
- 2MASS J2244 (L6.5, $p_{\rm da} = (2.5 \pm 0.5)\%$ in the I-band), however, is an extreme case that could only be simulated if:
  1. $T_{\rm eff}$ was less than $\sim 1500\,{\rm K}$. Estimated temperature: $1100\,{\rm K}$ ($1000\,{\rm K}$-$1200\,{\rm K}$) Stephens et al. (2009)

Preliminary interpretation of polarimetric observations

- Comparisons with 7 BD observations for which polarimetric measurements were available
- Most cases had intermediate values that would require more sophisticated retrieval methods to fit (subject to constraints available)
- 2MASS J2244 (L6.5, $p_{\rm da} = (2.5 \pm 0.5)\%$ in the I-band), however, is an extreme case that could only be simulated if:
  1. $T_{\rm eff}$ was less than $\sim 1500\,$K. Estimated temperature: 1100 K (1000 K-1200 K) Stephens et al. (2009)
  2. Nearly edge-on geometry.

Preliminary interpretation of polarimetric observations

- Comparisons with 7 BD observations for which polarimetric measurements were available
- Most cases had intermediate values that would require more sophisticated retrieval methods to fit (subject to constraints available)
- 2MASS J2244 (L6.5, $p_{\rm da} = (2.5 \pm 0.5)\%$ in the I-band), however, is an extreme case that could only be simulated if:
  1. $T_{\rm eff}$ was less than $\sim 1500\,$K. Estimated temperature: 1100 K (1000 K-1200 K) Stephens et al. (2009)
  2. Nearly edge-on geometry. Estimated inclination angle: $76^{+14}_{-20}{}^{\circ}$ (Vos et al. 2018)

Preliminary interpretation of polarimetric observations

- Comparisons with 7 BD observations for which polarimetric measurements were available
- Most cases had intermediate values that would require more sophisticated retrieval methods to fit (subject to constraints available)
- 2MASS J2244 (L6.5, $p_{\rm da} = (2.5 \pm 0.5)\%$ in the I-band), however, is an extreme case that could only be simulated if:
  1. $T_{\rm eff}$ was less than $\sim 1500\,$K. Estimated temperature: 1100 K (1000 K-1200 K) Stephens et al. (2009)
  2. Nearly edge-on geometry. Estimated inclination angle: $76^{+14}_{-20}{}^{\circ}$ (Vos et al. 2018)
  3. Thick clouds bearing fine-sized grains.

Preliminary interpretation of polarimetric observations

- Comparisons with 7 BD observations for which polarimetric measurements were available
- Most cases had intermediate values that would require more sophisticated retrieval methods to fit (subject to constraints available)
- 2MASS J2244 (L6.5, $p_{\rm da} = (2.5 \pm 0.5)\%$ in the I-band), however, is an extreme case that could only be simulated if:
  1. $T_{\rm eff}$ was less than $\sim 1500\,$K. Estimated temperature: 1100 K (1000 K-1200 K) Stephens et al. (2009)
  2. Nearly edge-on geometry. Estimated inclination angle: $76^{+14}_{-20}{}^{\circ}$ (Vos et al. 2018)
  3. Thick clouds bearing fine-sized grains. McLean et al. (2003) observed extreme reddening in the NIR

Preliminary interpretation of polarimetric observations

- Comparisons with 7 BD observations for which polarimetric measurements were available
- Most cases had intermediate values that would require more sophisticated retrieval methods to fit (subject to constraints available)
- 2MASS J2244 (L6.5, $p_{\rm da} = (2.5 \pm 0.5)\%$ in the I-band), however, is an extreme case that could only be simulated if:
  1. $T_{\rm eff}$ was less than $\sim 1500\,$K. Estimated temperature: 1100 K (1000 K-1200 K) Stephens et al. (2009)
  2. Nearly edge-on geometry. Estimated inclination angle: $76^{+14}_{-20}{}^{\circ}$ (Vos et al. 2018)
  3. Thick clouds bearing fine-sized grains. McLean et al. (2003) observed extreme reddening in the NIR
  4. High oblateness.

Preliminary interpretation of polarimetric observations

- Comparisons with 7 BD observations for which polarimetric measurements were available
- Most cases had intermediate values that would require more sophisticated retrieval methods to fit (subject to constraints available)
- 2MASS J2244 (L6.5, $p_{\rm da} = (2.5 \pm 0.5)\%$ in the I-band), however, is an extreme case that could only be simulated if:
  1. $T_{\rm eff}$ was less than $\sim 1500\,$K. Estimated temperature: 1100 K (1000 K-1200 K) Stephens et al. (2009)
  2. Nearly edge-on geometry. Estimated inclination angle: $76^{+14}_{-20}{}^{\circ}$ (Vos et al. 2018)
  3. Thick clouds bearing fine-sized grains. McLean et al. (2003) observed extreme reddening in the NIR
  4. High oblateness. McLean et al. (2003), Martin et al. (2017) classify 2M2244 as a V-LG object, hence more susceptible to deformation

Preliminary interpretation of polarimetric observations

- Comparisons with 7 BD observations for which polarimetric measurements were available
- Most cases had intermediate values that would require more sophisticated retrieval methods to fit (subject to constraints available)
- 2MASS J2244 (L6.5, $p_{\rm da} = (2.5 \pm 0.5)\%$ in the I-band), however, is an extreme case that could only be simulated if:
  1. $T_{\rm eff}$ was less than $\sim 1500\,$K. Estimated temperature: 1100 K (1000 K-1200 K) Stephens et al. (2009)
  2. Nearly edge-on geometry. Estimated inclination angle: $76^{+14}_{-20}{}^{\circ}$ (Vos et al. 2018)
  3. Thick clouds bearing fine-sized grains. McLean et al. (2003) observed extreme reddening in the NIR
  4. High oblateness. McLean et al. (2003), Martin et al. (2017) classify 2M2244 as a V-LG object, hence more susceptible to deformation
  5. High oblateness.

Preliminary interpretation of polarimetric observations

- Comparisons with 7 BD observations for which polarimetric measurements were available
- Most cases had intermediate values that would require more sophisticated retrieval methods to fit (subject to constraints available)
- 2MASS J2244 (L6.5, $p_{\rm da} = (2.5 \pm 0.5)\%$ in the I-band), however, is an extreme case that could only be simulated if:
  1. $T_{\rm eff}$ was less than ~ 1500 K. Estimated temperature: 1100 K (1000 K-1200 K) Stephens et al. (2009)
  2. Nearly edge-on geometry. Estimated inclination angle: $76^{+14}_{-20}{}^{\circ}$ (Vos et al. 2018)
  3. Thick clouds bearing fine-sized grains. McLean et al. (2003) observed extreme reddening in the NIR
  4. High oblateness. McLean et al. (2003), Martin et al. (2017) classify 2M2244 as a V-LG object, hence more susceptible to deformation
  5. High oblateness. Rotational period of 4.6h (Morales-Caldern et al. 2006), 11$\pm$2h (Vos et al. 2018)

Table of Contents

Summary

- Gravitational darkening can significantly amplify the polarization due to oblate BDs, allowing for the first time polarimetric measurements of over 2% to be simulated
- DoP increases with increasing oblateness and inclination angle (edge-on viewing is most polarizing)
- Optically thick clouds cause more dimming, small cloud grains cause reddening of the SED
- Polarization due to small grains is most effective at optical-NIR wavelengths
- Effects of atmospheric opacity need to be accounted for, especially for simulations of T-dwarfs: work currently underway - inputs and advice welcome!

Copyright 2019 California Institute of Technology. Government sponsorship acknowledged.